TRANSCRIPTOMIC ANALYSIS OF COBALT STRESS IN THE MARINE YEAST *DEBARYOMYCES HANSENII*

By

Yariela Gumá Cintrón

A thesis submitted in partial fulfillment of the requirements for the degree of
MASTER IN SCIENCE
In
MARINE SCIENCES
BIOLOGICAL OCEANOGRAPHY
UNIVERSITY OF PUERTO RICO
MAYAGÜEZ CAMPUS
2015

Approved by:

_____	_____
Govind S. Nadathur, Ph.D. President, Graduate Committee	Date
_____	_____
Nikolaos Schizas, Ph.D. Member, Graduate Committee	Date
_____	_____
Arup Sen, Ph.D Member, Graduate Committee	Date
_____	_____
Kurt A. Grove, Ph.D. Graduate School Representative	Date
_____	_____
Ernesto Otero Morales, Ph.D. Interim Director of Department	Date

ABSTRACT

Debaryomyces hansenii is a very versatile marine yeast capable of thriving under extreme conditions. Particularly important studies performed on this yeast include studies on osmotolerance and heavy metal resistance of various strains. With respect to its capability to survive when exposed to high concentrations of the heavy metal cobalt (Co (II)), strain J6 revealed to be highly tolerant. In an attempt to elucidate the mechanisms that activate in order to survive toxic exposure to heavy metals, microarrays of J6 were performed. This revealed that J6 was largely divergent from the type strain's, 767, genome. Given that the only available genome was that of the type strain, another approach needed to be taken in order to understand how J6 survives exposure to heavy metals. For this reason, a transcriptomic study was needed.

By sequencing J6's RNA after exposure to Co (II) in a time series experiment and comparing it to a control sample, identification of possible products, given that RNA can be used as a proxy for proteins, can thus allow us to identify the function of genes that are turned on and off during exposure. This analysis will provide information on the survival or adaptation mechanisms that J6 has developed. In order to elucidate such mechanisms, various steps need to

be followed: (i) identify the concentration of soluble cobalt that reduced the yeast cell density by half (this will give maximum response to stress), (ii) RNA sequencing, (iii) data processing and mapping to other similar yeast genomes, (iv) bioinformatics, in order to allocate biological function to each identified gene and elucidate survival mechanisms, and (v) validation of RNA sequencing data.

As a result of this study we were able to identify highly upregulated genes under heavy metal stress conditions to mainly fall into the following categories: (i) DNA damage and repair genes, (ii) oxidative stress response genes, and (iii) genes for cell wall integrity and growth. The main response of *D. hansenii* when in heavy metal stress is the activation of non-enzymatic oxidative stress response mechanisms and the control of biological production of reactive oxygen species. Our results indicate that although J6 does not seem to be preadapted to survive high heavy metal concentrations, its survival and detoxifying mechanisms are enough for the cells to recover quickly after heavy metal stress conditions.

RESUMEN

Debaryomyces hansenii es una levadura marina muy versátil, capaz de prosperar bajo condiciones extremas. Estudios particularmente importantes realizados con varias cepas de esta levadura incluyen estudios sobre osmotolerancia y resistencia a metales pesados. Con respecto a su capacidad para sobrevivir cuando se expone a altas concentraciones del metal pesado cobalto (Co (II)), la cepa J6 reveló ser altamente tolerante. En un intento de elucidar los mecanismos que se activan en J6 con el fin de sobrevivir a la exposición tóxica a metales pesados, se realizó un estudio de microarreglos. Esto reveló que J6 era en grandemente divergente al genoma de 767, la cepa tipo. Teniendo en cuenta que el único genoma disponible era el de la cepa tipo, fue necesario adoptar otro enfoque con el fin de entender cómo J6 sobrevive la exposición a metales pesados. Por esta razón, se necesitó un estudio de transcriptómica.

Con la secuenciación del ARN de J6 después de la exposición a Co (II) en un experimento de series de tiempo en comparación con una muestra control, permite la identificación de posibles productos, dado que el ARN puede ser utilizado como un proxy para proteínas, lo que nos puede permitir identificar la función de genes que están activados o desactivados como reacción a la

exposición a cobalto. Este análisis proporcionará información sobre los mecanismos de supervivencia o de adaptación que J6 ha desarrollado. Con el fin de elucidar estos mecanismos se deben seguir los siguientes pasos: (i) identificar la concentración de cobalto soluble que reduce la densidad de las células de levadura a la mitad (esto nos permitirá ver la máxima respuesta al estrés), (ii) secuenciación del ARN, (iii) procesamiento de datos y "mapping" a otros genomas de levadura similares, (iv) bioinformática, con el fin de asignar la función biológica de cada gen identificado y elucidar los mecanismos de supervivencia, y (v) validación de los datos de secuenciación de ARN.

Como resultado de este estudio hemos sido capaces de identificar los genes altamente regulados bajo condiciones de estrés por exposición a metales pesados, los cuales caen principalmente en las siguientes categorías: (i) daño y reparación del ADN, (ii) genes de respuesta al estrés oxidativo, y (iii) genes para la integridad de la pared celular y el crecimiento. La principal respuesta de *D. hansenii* bajo condiciones de estrés por exposición metales pesados es la activación de mecanismos no enzimáticos como respuesta al estrés oxidativo y el control de la producción biológica de especies reactivas de oxígeno. Nuestros resultados indican que aunque J6 no parece estar preadaptada a sobrevivir concentraciones altas de metales pesados, sus mecanismos de supervivencia y

desintoxicación son suficientes para que las células se recuperan rápidamente después de estas condiciones de estrés.

COPYRIGHT

Pa

ACKNOWLEDGEMENTS

This research was financially supported by RISE 2BEST UPRM, grant number NIH-R25GM088023 from the National Institute of General Medical Sciences. I am deeply grateful for the program's support, as well as for their staff members, Mairim Romero and Rosaly Ramos. This research would not have been successful if not for the National Center for Genome Resources (NCGR) in partnership with the Gordon and Betty Moore Foundation's Marine Microbiology Initiative (MMI) and Community Cyberinfrastructure for Advanced Microbial Ecology Research and Analysis (CAMERA) giving our lab the opportunity to participate in the Marine Microbial Eukaryote Transcriptome Sequencing Project (MMETSP). Also, I am very grateful for the help received by Arpan Bandyopadhyay and Dr. Wei Shou-Hu from the University of Minnesota, Twin Cities. Without their training and guidance, sequence analysis would have been impossible.

I would like to express my gratitude to my thesis advisor and the Molecular Marine Biology lab members, past and present; Govind, Bill, Vilma, and María: your knowledge, help, advice, conversations (academic and non-academic), and

friendship was very meaningful and important in my time as a graduate student and will carry on afterwards.

To my family and friends, your unconditional support is always appreciated. Thank you.

TABLE OF CONTENTS

LIST OF TABLES

LIST OF FIGURES

CHAPTER 1 –INTRODUCTION

Debaryomyces hansenii is a highly diverse and versatile yeast (Arroyo et al., 2009, Breuer et al., 2006, Seda-Miró, 2007) which has been isolated from a wide variety of substrates and has even been found in human infections (Desnos-Ollivier et al., 2008). Breuer et al. (2006) classify it as an extremophilic yeast given its osmotolerance, its presence in low-water-activity products, its capability to grow in high sugar containing media, and it high tolerance of heavy metals (Breuer et al., 2006, Prista et al., 1997, Seda-Miró et al., 2007). Its halotolerance has been widely studied given that it can grow in media with up to 4M NaCl, and the availability of the complete sequence of *D. hansenii* 767^{T} has made it possible to elucidate and understand the pathways for survival under extreme conditions (Arroyo et al., 2009).

Gadd and Edwards (1986) described *D. hansenii* as a flavinogenic yeast given that riboflavin overproduction was observed in the presence of heavy metals. A mutant strain of its anamorph, *Candida famata*, is in fact used industrially for the production of riboflavin (Breuer et al., 2006, Sibirny and Voronovsky, 2009). Heavy metals are trace elements needed for proper biological function of

metabolic and signaling pathways; because their *d* orbital is incomplete these metals can act as cofactors (Valko et al., 2005). Nevertheless, the same function they have in trace levels becomes toxic at higher concentrations given their high redox activity and strong binding potential (Valko et al., 2005). These high levels of heavy metals induce toxicity and inhibit normal physiological processes (Nies, 1999). For this reason, intracellular concentrations of heavy metals has to be tightly regulated (Nies, 1999).

In their study, Seda-Miró et al. (2009) proposed the use of *Debaryomyces hansenii*, strain J6 as a heavy metal biosensor given that it survives exposure to toxic concentrations of cobalt and produces riboflavin as a direct response to this exposure, which can be monitored by the appearance of a yellow pigment. However, even though riboflavin was produced in a direct relationship to cobalt concentration in the media, yellow pigment could not be directly observed in the media until after 72 hours after exposure (Seda-Miró et al., 2009). For this reason, a comprehensive study of the mechanisms of survival when J6 is exposed to sub-lethal concentrations of soluble cobalt was needed as a pre-requisite for the identification of a possible reporter gene, with a much rapid response. As a first attempt, a microarray of J6 after exposure to cobalt was performed, only to realize that J6's sequence was highly divergent from that of 767^{T} (unpublished data). Even

though a trancriptomic study with microarray was hindered by the large heterogeneity between strains of *D. hansenii,* with the availability of next generation sequencing, a new approach could be taken.

RNA sequencing (RNA-Seq) provides data directly from functional genomic elements and can be used to assess function under a set condition, given that RNA, and thus protein synthesis, can be used as a proxy for function (Wolf et al., 2013). Quantification of genes may be calculated by ways of the expression or abundance of each gene (Aurer et al., 2010, Marioni et al., 2009, Wolf et al., 2013). Many studies have used RNA-Seq as a tool to elucidate the mechanisms by which different organisms or tissues survive stress conditions. It is the purpose of this study to understand which are the mechanisms of survival and/or adaptation that *Debaryomyces hansenii* J6 employs in order to survive exposure to toxic levels of cobalt.

CHAPTER 2 - LITERATURE REVIEW

2.1 Heavy Metal Contamination- Case Study: Cobalt

The heavy metal cobalt is a natural Earth element that is found in trace amounts in the environment and in its stable form is present as a +II oxidation state metal (Gault et al., 2010, Valko et al., 2005). Cobalt, as well as other transition metals, is an important cofactor required for normal biological function and can be found in foods and especially in vitamin B12 (Nies, 1999, Valko et al., 2005). Apart from its dietary consumption, natural cobalt exposure levels are relatively low. Higher, contaminating levels may be created in industrial settings given that cobalt is very common in alloys and hard metals, is released by the burning of coal and oil, and its salts are largely used in paints and pigments (Gault et al., 2010, Valko et al., 2005). The dangers of cobalt exposure at levels above those required biologically lies on its genotoxic characteristics; reactive oxygen species (ROS) as formed as a consequence of cobalt absorption by cells (Valko et al., 2005). Pearce and Sherman (1999) studied the production of hydroxyl radicals in *Saccharomyces cerevisiae* after exposure to copper, cobalt, and nickel salts. Gault et al. (2010) also performed a study in which they exposed the

HaCaT keratinocyte cell line to different levels of the cobalt salt $CoCl_2$. They found that genotoxic damage was time and dose dependent and that cell viability was reduced to EC_{50} when exposed to cobalt concentrations in the range of 690-850μM.

Most marine ecosystems are recognized as anthropogenically stressed. Thus, contamination in these environments is very common, with the main impact caused by organic substances, heavy metals and hydrocarbons (Chi et al., 2010). Detection of heavy metal contamination in water and sediments is usually hindered by the fact that many of these metals are in concentrations that fall below analytical detection and are temporal (Rainbow, 1995). In a recent review of mangrove ecosystem and the impact of anthropogenic chemicals, Lewis et al. (2011) gathered seven reports of accumulation of cobalt in mangrove sediments and 5 reports of accumulation of cobalt in mangrove plant tissue. Although by the time of their review there were no reports for accumulation of cobalt in mangrove ecosystems of Puerto Rico, other heavy metals have been reported as follows: Cu (2.1-49μg/g dry sediment), Hg (200, 400ng/g dry sediment), Mn (420-1100μg/g dry sediment), Ni (47-75 μg/g dry sediment), and Zn (69-160 μg/g dry sediment) (Lewis et al., 2011).

2.2 *Debaryomyces hansenii* as a Cobalt Biosensor

Debaryomyces hansenii is an easily cultivated marine Ascomycete yeast with a wide range of extremophilic behavior- its ability to grow in up to 24% w/v NaCl is one that stands out (Arroyo et al., 2009). This species is highly heterogeneous (Breuer et al., 2006; Seda-Miró et al., 2007) with high sequence divergence among strains, evidence of which is found in their large variability in 26S rRNA (Breuer et al., 2006). Although the complete genome of the type strain CBS 767^T has been sequenced, strain J6 has been identified in previous studies to overproduce riboflavin approximately 72 hours after exposure to high concentrations of Co (II) in a fashion proportional to the concentration of cobalt in the medium (Seda-Miró et al., 2007). In this study, 34 different *D. hansenii* strains where exposed to sublethal levels of Co (II) concentrations, out of which ~65% were found to be highly tolerant or tolerant, including the flavinogenic strain J6 (Seda-Miró, 2012). It was observed that when this strain was exposed to Co (II) at a concentration of 0.5mM, there was a growth inhibition of approximately 40% with an observable increase in the acclimation period of the cells (Seda-Miró et al., 2012). However, these experiments were not performed under the conditions where the cells are exposed to the metal at different stages

of growth. It is also logical to believe that the mortality rates of cells would depend on the number of cells exposed to the metal.

Debaryomyces hansenii has been found in abundance in marine shallow water environments, marine sediments, and in estuaries (Kutty et al., 2008), making *D. hansenii* a potential biosensor for heavy metal contamination, specifically Co (II), in marine environments. A phenotypic evaluation of the growth *D. hansenii* exposed to toxic levels of cobalt was performed, but a genotypic evaluation is lacking. For this, a comprehensive study and analysis of the global genetic response of *D. hansenii* to metal (oxidative) stress will provide the information needed to identify possible reporter genes that will make *D. hansenii* an ideal biosensor for cobalt contaminated marine environments.

2.3 Why Transcriptomics? - RNA-Seq

The use of riboflavin overproduction as a correlation to Co(II) in the medium is not a reliable physiological/biochemical change for the use of *D. hansenii* as a heavy metal biosensor given that the visible and measurable production of riboflavin after exposure to Co(II) takes too long for practical applications. The initial attempt to use microarrays to identify differential expression patterns in J6 failed due to the high sequence divergence between J6

and the annotated CBS 767^{T} (unpublished data). On the other hand, RNA sequencing gives data that is directly derived from functional protein coding genes (the transcriptome) (Wolf et al., 2013). The transcriptome gives complete information about the function and quantity of the expressed genes (mRNA) at specific developmental stages or conditions (Marioni et al., 2009; Wolf et al., 2013). On the other hand, microarrays are limited in that their detection levels are limited, previous knowledge of the genome is needed, a priori assumptions must be made, and sequence divergence must be low given that the procedure requires cross-hybridicazion of experimental cDNA to DNA from a reference (Aurer et al., 2010; Marioni et al., 2009).

CHAPTER 3 – METHODOLOGY

3.1 Assessing Sublethal Co (II) Concentrations

Debaryomyces hansenii strain J6 was used in this study based on its ability to survive when exposed toxic of concentrations of Co (II). The strain was isolated from a Swedish estuary and gifted by Dr. Adler of the University of Gothenburg, Sweden. As per Seda-Miró et al. (2007), when *D. hansenii* J6 was grown directly on cobalt containing media, cell density was reduced approximately to half of that of the control culture when cobalt concentration was at 0.5mM. However, in order to assess all the possible resistance mechanism of the cell, gene inhibition due to high glucose concentration in the media had to be eliminated. For that reason, J6 was exposed to cobalt at late log phase. Given the growth phase and the cell density, the concentration of cobalt that would reduce the cell density in half was assessed. A yeast culture was prepared, which contained 250mL of YPD (1% yeast extract, 2% peptone, 2%dextrose). The culture was placed in an orbital shaker (150 rpm) at 25°C until late log phase was reached (A_{600}=9.5-10). Once late log phase was reached samples were diluted to 10^8 with distilled water and cell number was counted using an hemocytometer. Immediately after the control cells were collected, 5mM Co (II) ($CoSO_4 \cdot 5H_2O$) was added. Samples were collected and cell

number was counted 0.5, 1.5, and 3-h after exposure to cobalt following the same procedure as before. Cell death was calculated as the ratio of cell number in each treatment to the cell number of the control (0-h).

3.2 Growth Conditions

Growth conditions of J6 were assessed. A concentration of 5mM Co (II) was chosen for transcriptomic analysis as it represented a condition of high stress to the cells. J6 was grown to late log phase as previously shown and control samples were collected, centrifuged (5 min at 6K rpm), washed two times with distilled water, flash frozen, and stored at -80°C. Immediately after the cells were collected, 5mM Cobalt (II) ($CoSO_4 \cdot 5H_2O$) was added to the remaining culture, which was kept in the orbital shaker at 25°C. Following the same procedure as before, samples of J6 exposed to Co (II) were collected at 0.5, 1.5, and 3-h intervals.

3.3 RNA Extraction, Library Construction, RNA-seq, and Mapping

Total RNA was isolated using the RNeasy Mini Kit (Qiagen, CA, USA) with an on-column DNase treatment as indicated by the manufacturer. RNA

concentration was determined by measuring absorbance at 260nm (Genesis 10S UV-Vis, Thermo Scientific), purity was analyzed by the ratio of readings at 260nm and 280nm (A_{260}/A_{280}), and integrity was checked with an agarose gel electrophoresis. RNA samples were sent to the National Center for Genome Resources (NCGR) (Santa Fe, NM, USA), as part of the Marine Microbial Eukaryote Transcriptome Sequencing Project (MMETSP), where mRNA enrichment, cDNA library preparation, adapter addition, size selection (250-350bp), PCR and RNA-seq (Illumina HiSeq™ 2000) were performed (Keeling et al., 2014). Pre-assembly quality and quality trimming was also performed at NCGR with a cut-off at Q15 (as described by Keeling et al., 2014). The resulting RNA-seq reads were mapped to *D. hansenii* 767 (GCA_000006445.2) using Burrows-Wheeler Alignment (v 0.5.9) (Li et al., 2009) allowing for three mismatches per 100 bp read. The mapped reads were filtered to remove reads mapping to more than two positions in the genome. The transcriptome may be accessed through the CAMERA Data Distribution Center (http://camera.crbs.ucsd.edu/mmetsp/) and in the Sequence Read Archive (SRA) under BioProject PRJNA231566.

3.4 Gene Expression and Functional Annotation

Using Artemis, the number of mapped reads of each gene was quantified and normalized into RPKM (reads per kb per million reads). To adjust for the variability in sequencing depth using the upper quantile normalization procedure (Bullard et al., 2010). Fold change in gene expression was calculated as $\log_2$ ratios with respect to the control sample (0-h). Expression profiles (functional clusters) were obtained with Spotfire DecisionSite v. 9.1.1 by k-means clustering. Using only those genes that had a four-fold or more change in expression at any given time point six clusters were identified. These genes were assigned IDs from UniProt protein database, Ensembl (EMBL-EBI and Wellcome Trust Sanger Institute) and the *Candida* Genome Database (Inglis et al., 2012). Gene ontology (GO) classification was obtained through the Gene Ontology Consortium (Ashburner et al., 2000). Functional clustering of those genes was done using DAVID to extract biological meaning from the large gene/protein list.

3.5 Validation by qRT-PCR

Total RNA for qRT-PCR was extracted as mentioned above. Two genes with induced expression were identified (DEHA2F05742G (Histidinol-phosphate

aminotransferase) and DEHA2D13772G (ATP phosphoribosyltransferase)) and primers were designed for quantitative real time PCR (qRTPCR) (Table 3-1). Actin (ACT1, Accession No. XM_45873) from *D. hansenii* CBS767 was used as the normalizing gene (Dujon et al., 2004). qRT-PCR was performed as a 1-step reaction using Brilliant II SYBR® Green QRT-PCR Master Mix Kit (Agilent Technologies, Santa Clara, CA, USA) in the Mx3005P analyzer (Stratagene, La Jolla, CA, USA). The qRT-PCR mixture (25µl total per well) consisted of 12.5µl of SYBR® Green QRT-PCR master mix, 0.25pmol/µl of each primer for gene Histidinol-phosphate aminotransferase, 0.250pmol/µl forward, 0.50pmol/µl reverse for gene ATP phosphoribosyltransferase, and 0.50pmol/µl of each primer for actin; 0.375µl of the reference dye (ROX diluted 1:500), 1µl of RT/RNase block enzyme mixture, 350ng of total RNA and RNase-free water to adjust the final volume to 25µl. The cycling protocol was performed as a three-step method, which was initiated at 50°C for 30 minutes (reverse transcription step), 95°C for 10 minutes, the 40 cycles of 95°C for 30 seconds, 50°C (for all three primers) for 1 minute, and 72°C for 30 seconds. Specificity of the primers was confirmed with a dissociation curve which initiated at 95°C for 1 minute, 55°C for 30 seconds and then a ramp in temperature to 95°C with a data acquisition at a rate of 0.2°C/s). To calculate gene abundance, the $\Delta\Delta C_T$ method was applied.

Table 3-1: Primer information for genes used in qRT-PCR as an RNAseq validation method.

Gene	Forward primer (5′ to 3′)	Reverse primer (5′ to 3′)	Product size (bp)	T_m (°C)
Histidinol-phosphate transaminase	CTTTCAGATAGATGTGGATG	GATTCACTAGATGTTTCAC	222	55.5 (Fwd) and 53.2 (Rev)
ATP phosphoribosyltransferase	GATTTAGTTGAAAGTGGTGA	AATAGTTGCAGATCTTCTA	248	55.8 (Fwd) and 53.3 (Rev)
Actin	GATTATGAAGTGTGATGTC	TTAGAAACACTTATGATGAAC	286	53.1 (Fwd) and 54 (Rev)

CHAPTER 4 - RESULTS

4.1 Cell Survival Upon Exposure to Cobalt

Our study shows that even though exposure to 0.5mM Co (II) reduces cell densities by 40% when they are grown directly on cobalt containing media, an approximation to D_{50} is observed when the cells are in late log phase and exposed to a cobalt concentration ten times that of the original study. Specifically, exposure to 5mM Co (II) at late log phase reduces cell density between 55, 67 and 66%, as seen in Figure 4-1.

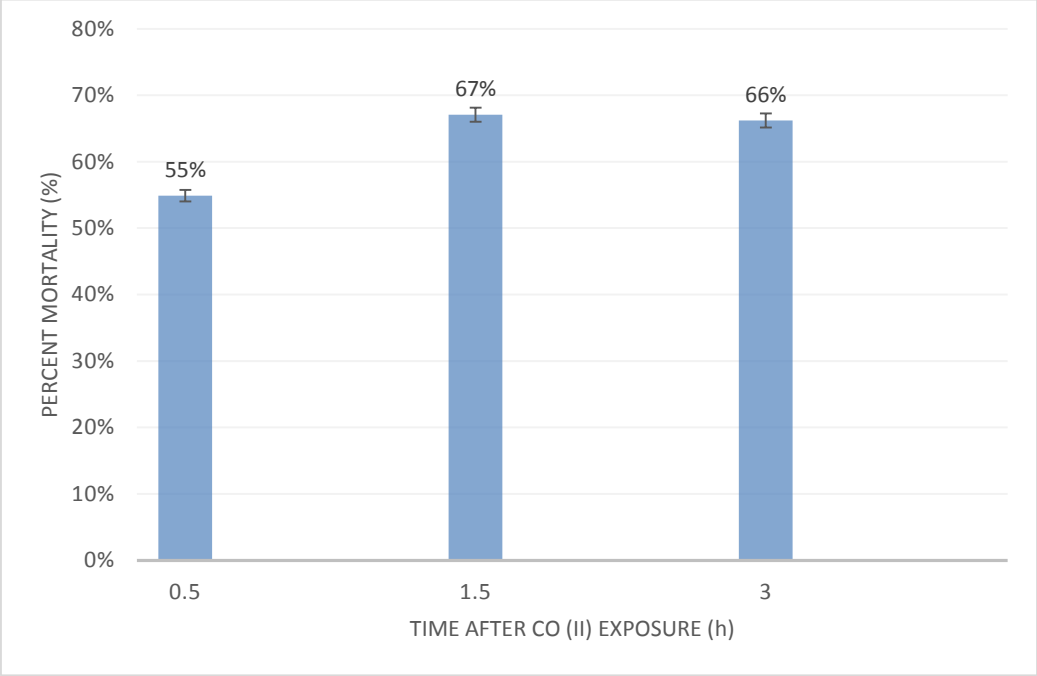

Figure 4-1: Percent mortality of J6 0.5, 1.5, and 3 hours after initial exposure to Co (II). Mortality rates calculated as cell count ratio of exposed cells to that of a control.

Given the approximation to D_{50} reached, this cobalt concentration was chosen to be used for transcriptomic analysis. RNA from control cells (0-h) and the time sequence experiment (0.5, 1.5, and 3-h) was successfully extracted, as seen in Figure 4-2 by the clear presence of the 28S, 18S, and 5.8S and 5S rRNA bands.

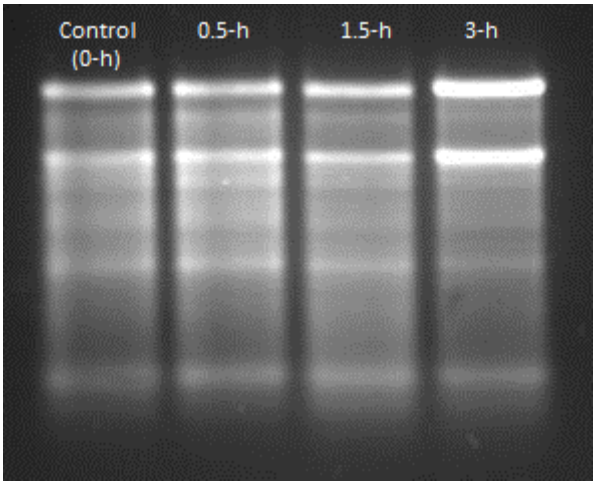

Figure 4-2: Denatured agarose gel electrophoresis of total RNA extracted from J6 at late log phase (0-h) and after exposure to 5mM Co (II).

4.2 RNA Sequencing and Differential Gene Expression

Paired-end sequencing of *D. hansenii* J6 RNA when exposed to 5mM Co (II) allowed the identification of a total of 4721 coding regions (17 Mb raw data), of which 471 had a fold change at any one time point of four or more as compared to the control (Figure 4-3).

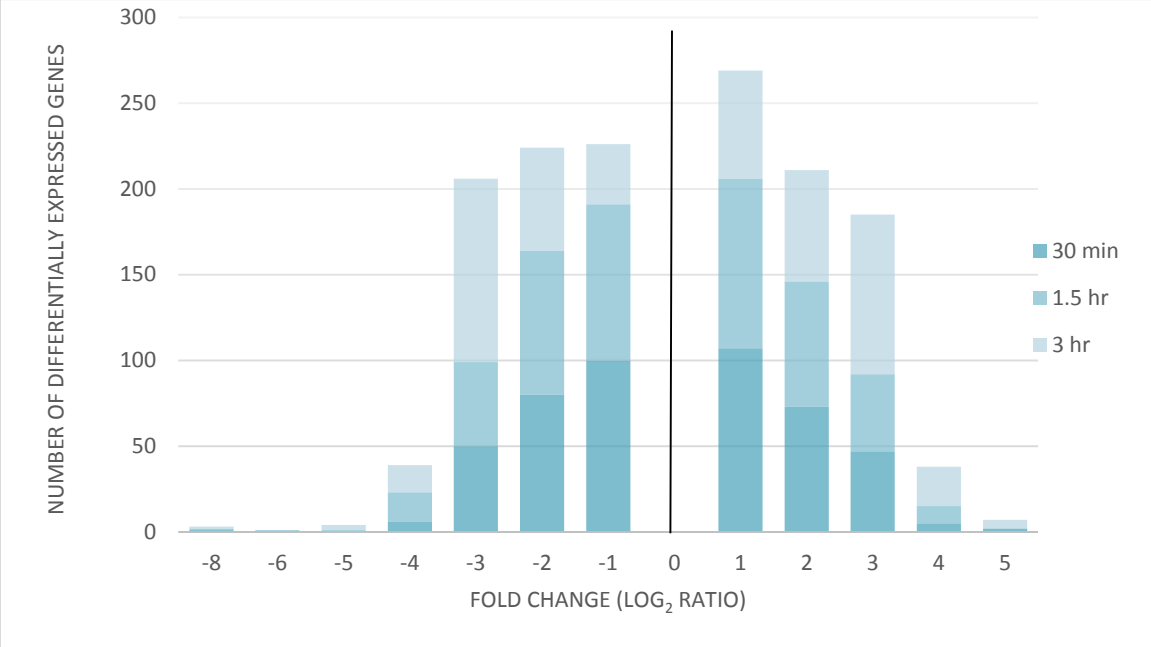

Figure 4-3: Temporal fold change of differentially expressed genes in J6 when exposed to 5mM Co (II).

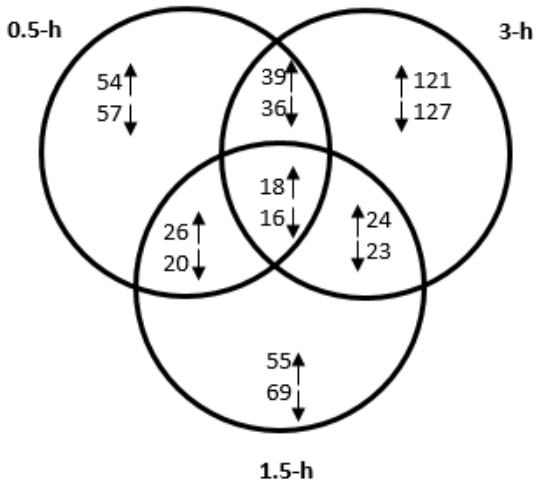

Figure 4-4: Venn diagram of the 471 genes with a fold change of four or more at any time point.

Approximately 40% of these genes were functionally annotated using the Uniprot public database, while the other 60% appear to be of unknown function. Among the 40% functionally annotated genes, 7% showed high homology, 67% showed homology and 26% showed weak homology to genes from the organisms that follow. Mapping and functional annotation revealed that approximately 58% of the identified genes have homologs to *Saccharomyces cerevisiae* and 20% to *Candida albicans*; the other 22% was homologous to other species, among them *Schizosaccharomyces pombe, Yarrowia lipolytica, Pichia stipites,* and *Aspergillus oryzae*. Figures 4-3 and 4-4 depict down- and upregulated oscillation between significantly expressed genes (at least four-fold change), where 0.5-h after exposure to cobalt 54 genes were upregulated, while 57 were downregulated; 1.5-h after exposure 55 genes were upregulated and 69 were downregulated; and 3-h after exposure 121 genes where upregulated while 127 gene were downregulated.

4.3 Temporal Trend and Gene Ontology

Six temporal trends where identified, in which 95 of the genes had a monotonically decreasing trend, 89 showed a monotonically decreased

expression with delayed response, 70 showed decrease followed by increase, 68 had an oscillating trend, 108 had a monotonically increasing response, and 41 showed an increase followed by a decrease (Clusters 1-6, respectively, in Figure 4-5, Table A-1).

Genes that were upregulated and downregulated at each time point were functionally clustered into the following categories: binding, cell part, transferase activity, molecular function, lipid metabolism, ion binding, amino acid metabolism, catalytic activity, physiological response to stimulus, transporter activity, oxidation-reduction process, protein metabolic process, carbohydrate metabolism, and biological process (Figure 4-6, Table A-1). Generally speaking, a noticeable trend is seen, where 30 minutes after the initial exposure to Co (II), cells had recovered by upregulating the expression of genes for DNA synthesis and repair, non-enzymatic oxidative stress response and upregulating metabolic pathways that lower the production of superoxide. This response was sustained at both 1.5 hours and three hours. After three hours of exposure to Co (II) recovery was accompanied by the upregulation of genes needed for cell division and mitosis. Genes for protein biosynthesis and ribosomal processes have been observed to be downregulated under stress conditions (Marks et al., 2008), for this reason details of these processes will not be discussed.

(a)

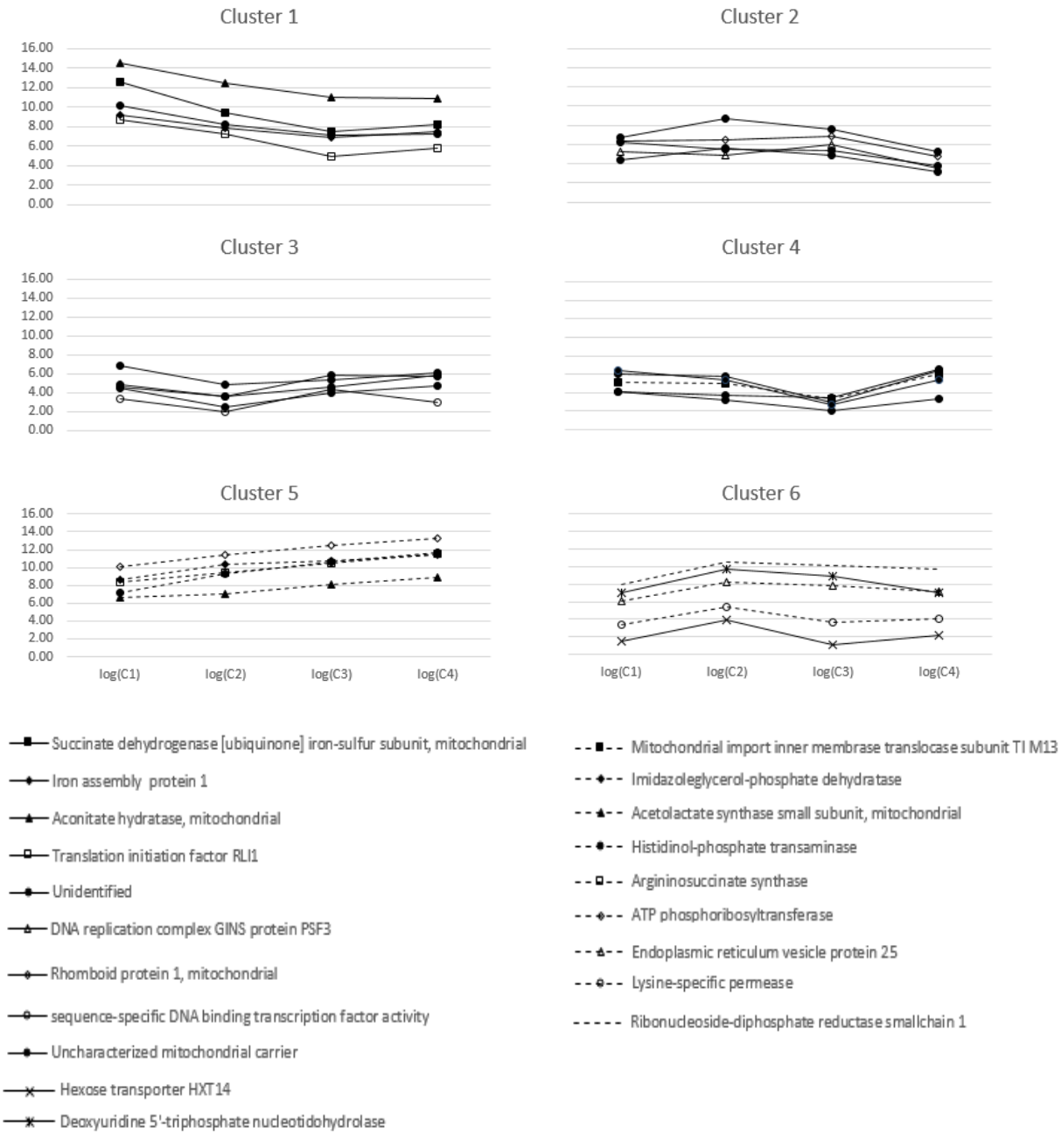
Cluster 1
Cluster 2
Cluster 3
Cluster 4
Cluster 5
Cluster 6
16.00
14.00
12.00
10.00
8.00
6.00
4.00
2.00
0.00
log(C1)
log(C2)
log(C3)
log(C4)
Succinate dehydrogenase [ubiquinone] iron-sulfur subunit, mitochondrial
Iron assembly protein 1
Aconitate hydratase, mitochondrial
Translation initiation factor RLI1
Unidentified
DNA replication complex GINS protein PSF3
Rhomboid protein 1, mitochondrial
sequence-specific DNA binding transcription factor activity
Uncharacterized mitochondrial carrier
Hexose transporter HXT14
Deoxyuridine 5'-triphosphate nucleotidohydrolase
Mitochondrial import inner membrase translocase subunit TI M13
Imidazoleglycerol-phosphate dehydratase
Acetolactate synthase small subunit, mitochondrial
Histidinol-phosphate transaminase
Argininosuccinate synthase
ATP phosphoribosyltransferase
Endoplasmic reticulum vesicle protein 25
Lysine-specific permease
Ribonucleoside-diphosphate reductase smallchain 1

(b)

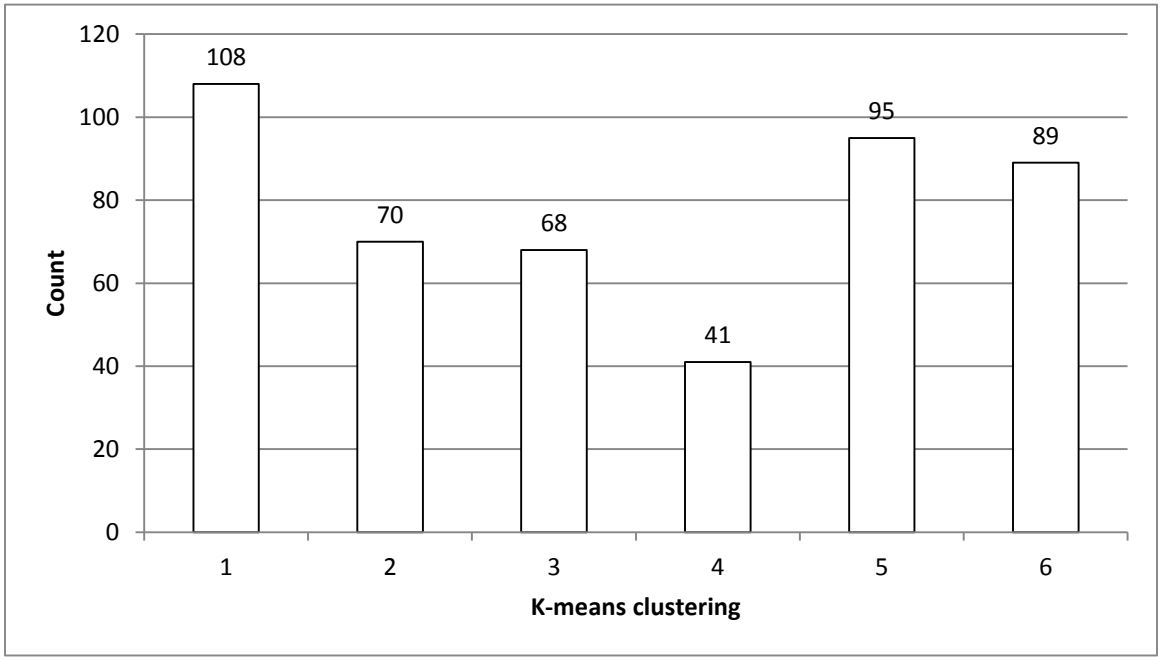

Figure 4-5: (a) Temporal trends of the 471 genes with a fold change (log base 2) of four or more. C1, C2, C3, and C4 correspond to 0-h, 0.5-h, 1.5-h, and 3-h, respectively. (b) Number of genes in each temporal cluster.

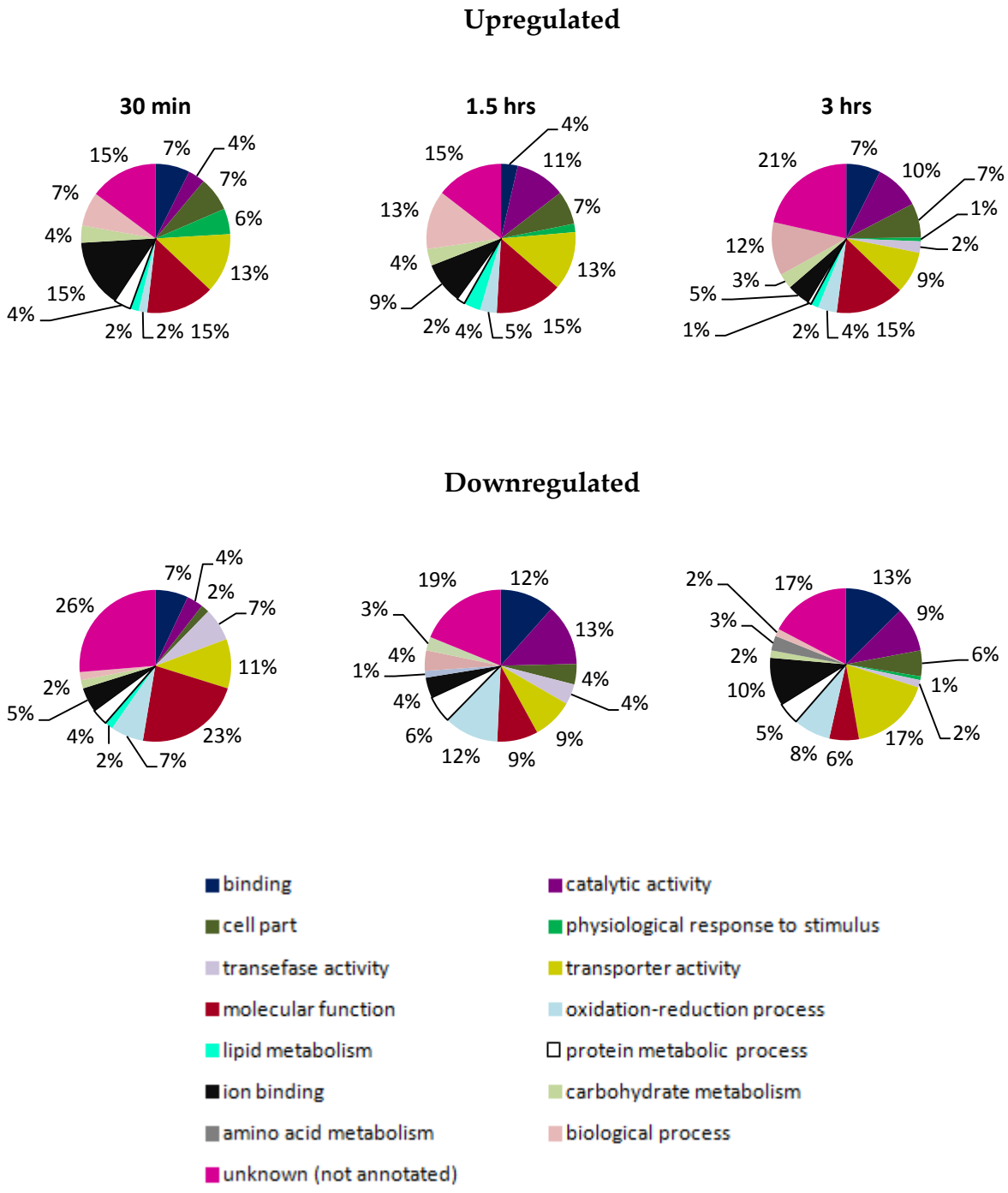

Figure 4-6: Temporal and functional gene expression of J6 when exposed to 5mM Co (II). Percentage of up- and downregulated genes based on function and calculated based on the number of genes with a fold change of four or more in each time point.

4.4 Functional Clusters

After analysis of J6's response to Co (II), it was found that its survival mechanisms are characterized mainly by the activation of genes for DNA synthesis and repair, oxidative stress response, and cell wall repair.

4.4.1 DNA Synthesis and Repair

Heavy metal toxicity is caused when cells are exposed to these in amounts larger than those biologically required; DNA cleavage at all bases is particularly caused by exposure to Co (II) (Valko et al., 2005). It is then expected that many of the genes over expressed as a result of cobalt exposure should be DNA repair genes. The majority of the upregulated genes 30 minutes after initial exposure to cobalt fall within the ion binding functional category (15%; Figure 4-6). These genes are in most part DNA synthesis and repair genes (Table A-1). DNA synthesis and repair genes continue to be upregulated throughout all time points, but with a decrease in the number of the genes expressed (Table A-1). There are also other DNA syntheses and repair genes that fall within the binding functional category over expressed at all three time points, in particular protein PLM2. PLM2 is a protein that binds to the promoter of genes involved in DNA synthesis and repair, chromosome segregation, nuclear division, and

transcription (Horak et al., 2002). Also within this functional category, and related to DNA synthesis and repair, genes for transcription activation, chromosome maintenance, and rRNA and snRNA biogenesis are upregulated (Table A-1). Within the catalytic activity functional cluster ribonuclease H2 subunit A, a DNA replication and repair gene (Jeong et al., 2004), is upregulated at the first 30 minutes after cobalt exposure (TableA-12). Also, protein SYM1, required to maintain mtDNA integrity and stability, if found to be upregulated at all three time points (Dallabona et al., 2010).

4.4.2 Oxidative Stress Response

Apart from causing DNA cleavage at all bases, Co (II) and all other heavy metals in quantities larger than those biologically needed cause oxidative stress by producing reactive radical species (Valko et al., 2005). Within the ion binding category and by the three hour time point, protein STB5 is over expressed. Protein STB5 has been identified as a mediator in oxidative stress response (Larochelle, M. et al., 2006). Amino acid metabolism genes that where upregulated throughout all three time points included the transcriptional activator protein UGA3 and glutathione S-transferase 1. The transcriptional activator protein UGA3 is a γ-aminobutyric acid (GABA)-dependent regulator

for the transcription of genes required for GABA catabolism (André, B., 1990) and glutathione is a known molecule that acts in non-enzymatic response to oxidative stress, acting as a radical scavenger (Jamieson, D.J., 1998). Within the TCA cycle and in the catalytic activity functional cluster, the gene coding for the enzyme aconitate hydratase is downregulated at all three time points. Tretter and Adam-Vizi (2000) demonstrated that this enzyme is sensitive to oxidative stress. Another TCA cycle and electron transport chain (complex II) enzyme downregulated was succinate dehydrogenase (TableA-1). Also, a component of complex I in the electron transfer chain, subunit NUHM, is downregulated at 1.5 and 3 hours after exposure to cobalt. Complex I and II have NADH dehydrogenase activity, which causes superoxide production, specifically at the quinine binding site in complex I (Lambert and Brand, 2004).

Other important genes that were upregulated at the last two time points include genes for the biosynthesis of lysine and histidine, which act in non-enzymatic oxidative stress response (Pearce and Sherman, 1999). Many of the genes upregulated in the transporter category were lysine and histidine specific as well as GABA specific amino acid permeases (GAP1; upregulated at the last two time points). BUL1, needed for polyubiquitination and intracellular trafficking of GAP1 (Bach et al, 2009), is upregulated at the first two time points,

then downregulated at the 3 hour mark (Table A-1). Within the functional cluster for oxidation-reduction process, sulfiredoxin, an enzyme activated in response to oxidative stress (Biteau et al, 2003), was found to be upregulated at the three hour time point. Another gene found to be upregulated in response to oxidative stress was LAG1 (lipid metabolism function), a ceramide synthesis component. Ceramides have been found to be induced under oxidative stress conditions (Van Brocklyn and Williams, 2012). Remarkably, *D. hansenii*'s response to oxidative stress is completely non-enzymatic and many enzymes that eliminate toxic radical species are downregulated at all three time points (Table A-1).

4.4.3 Cell Wall Integrity and Growth

Free radicals, produced as a consequence to heavy metal exposure, also affect cell membranes by oxidizing membrane lipids (Valko et al., 2005). Thus, upregulation of genes, which contribute to membrane repair is expected. During the first 1.5 hours of exposure to cobalt, proteins for maintenance and integrity of cell wall components are activated. What is remarkable is the upregulation of genes for cell division and growth are already overexpressed at 30 minutes after initial exposure to cobalt (Table A-1). The gene encoding Paxillin-like protein 1

(PXL1) is highly over expressed throughout the entire time series. PXL1 is a Rho-family GTPase required for vegetative growth and mating (Mackin, N. et al, 2004). Asexual reproduction by sporulation seems to be inhibited by exposure to cobalt given that a putative transcription factor involved in the sporulation process, SEF1 (Groom et al., 1997), is suppressed at all three time points. 30 minutes after exposure to Co (II) the cells are upregulating the expression of a karyogamy protein (KAR4), a chromatin assembly protein (chromatin assembly factor 1 subunit p90), and RNA polymerase I, and other genes within the cell part functional category (Table A-1). The chromatin assembly factor and the RNA polymerase I over expression is sustained at 1.5 hours. Also, a bud site selection protein (BUD4) is over expressed. This protein, in collaboration with PXL1, contributes to vegetative growth of the cell (Mackin et al., 2004). Also, within the carbohydrate metabolism category, GAS1 is found to be upregulated the first 30 minutes after cobalt exposure. GAS1 is a 1,3-beta-glucanosyltransferase.

4.5 Validation of RNA-Seq with qRT-PCR

Validation of the RNA-seq data by qRT-PCR revealed very similar trends within the chosen genes (Figure 4-7). The two genes used for qRT-PCR validation

were chosen for falling within the highest overall fold change in the monotonically increasing cluster. These two genes code for a Histidinol-phosphate transaminase and for an ATP phosphoribosyltransferase, with an overall fold change of 21.49 and 8.58, respectively. The enzyme Histidinol-phosphate transaminase catalyzes the formation of L-glutamate, an amino acid important in the GABA shunt pathway (Bach et al., 2009 and Coleman et al., 2001). On the other hand, the enzyme ATP phosphoribosyltransferase has a role in histidine metabolism which, as mentioned before, has a role in non-enzymatic oxidative stress response (Pearce and Sherman, 1999). Both enzymes are significant contributors in *D. hansenii*'s response to oxidative stress as a result of its exposure to subtoxic levels of Co (II), as will be discussed in the next chapter.

(a)

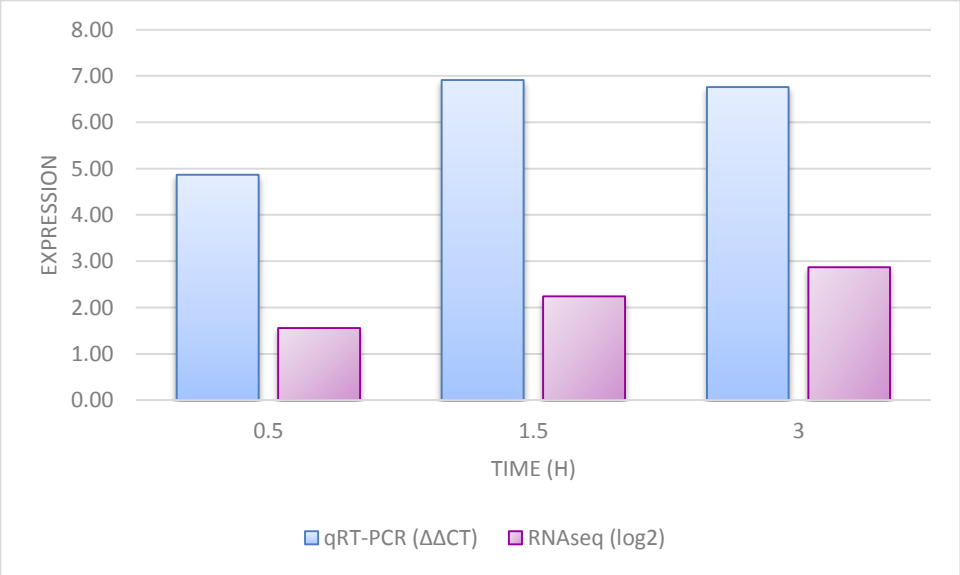

(b)

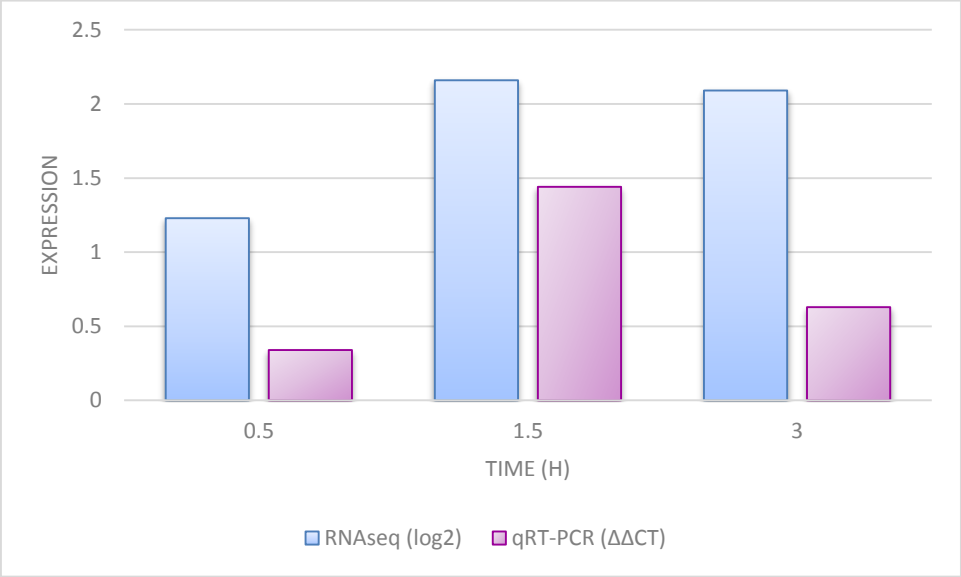

Figure 4-7: Comparison of qRT-PCR expression pattern with RNA-Seq fold change for (a) Histidinol-phosphate transaminase and (b) ATP phophoribosyltransferase.

CHAPTER 5 - DISCUSSION

5.1 DNA Synthesis and Repair

As mentioned above, Co (II) is known to cause genotoxic damage when cells are exposed to levels higher than those biologically required, as seen by the production of nucleobases in cells exposed to heavy metals such as cobalt (Valko et al., 2005). Heavy metals have the ability to produce reactive oxygen species, which oxidize DNA, lipids, proteins, and carbohydrates (Coleman et al., 2001; Valko et al., 2005). Overexpression of DNA repair genes (RAD52, DNA mismatch repair protein MSH2, SMC1, replication factor C subunit RFC5, MMS21, etc.) in response to cobalt exposure had a reduced expression with time, suggesting DNA damage repair (Table A-1). On the other hand, PML2, a gene involved in DNA synthesis and repair, chromosome segregation, nuclear division, and transcription regulation, showed a sustained increase in expression throughout the time points analyzed (Table A-1). PLM2 functions in DNA synthesis and repair when induced either at START in the cell cycle or upon DNA damage (Gasch et al., 2001; Horak et al., 2002). This gene is regulated periodically throughout the cell cycle, specifically during the G1/S transition (Horak et al., 2002). Also, SYM1 which has been shown to be activated during stress conditions

and is involved in maintaining structural and functional stability of the inner mitochondrial membrane, including mtDNA stability, was upregulated at all three time points Dallabona et al. (2010). Dallabona et al. (2010) demonstrated that *sym1*Δ mutants show a defect in electron transport chain components. These components play an important role in the oxidative stress response of *D. hansenii*, as will be discussed subsequently. This response is consistent with the observation of initial shock followed by recovery, with respect to DNA damage, as shown by the increase in upregulation of PLM2 and SYM1 throughout all three time points.

5.2 Oxidative Stress Response

NADH production and electron leaks to oxygen as they are being transported from reduced substrates to complex IV in the electron transport chain, form reactive oxygen species during normal metabolic processes (Jamieson et al., 1998; Lambert et al., 2004; Sulahian et al., 2006; Tretter and Adam-Vizi, 2000). Under heavy metal exposure, mitochondrial membrane potential can be reduced by the lack of NADH produced within the Krebs cycle since aconitase, α-ketoglutarate dehydrogenase (α-KGDH) and succinate dehydrogenase (SSADH) are highly

affected by oxidative stress (Tretter and Adam-Vizi, 2000). However, the loss of NADH can be compensated by the catabolism of γ-aminobutyric acid (GABA) and the GABA shunt pathway (Bach et al., 2009; Michaeli et al., 2001; Sulahian et al., 2006). The GABA shunt is a highly conserved pathway where decarboxylation of L-glutamate results in the production of GABA, which is then converted into succinate by means of glutamate decarboxylase (GAD), GABA transaminase, and succinate semialdehyde dehydrogenase (SSADH) (Bach et al., 2009; Coleman et al., 2001). These enzymes are encoded by GAD1, UGA1, and UGA2, respectively, which are induced by the transcriptional activator UGA3, a GABA-dependent regulator (André et al., 1990; Bach et al., 2009). The GABA shunt helps in recovering the loss in mitochondrial electron chain potential through the enzyme SSADH, which produces NADH or NADPH by oxidizing succinate semialdehyde into succinate (Coleman et al., 2001). Transcpitomic analysis of upregulated genes indicates that the TCA cycle in *D. hansenii* is highly affected by oxidative stress, but the affected steps are bypassed through the GABA shunt, as discussed below.

During exposure to Co (II), UGA3 was seen to be activated and over expressed at all three time points studied, with a decrease in expression with time, but always over a fourfold change (Table A-1). Also, the general amino acid

permease GAP1, which is GABA specific (André et al., 1990; Bach et al., 2009), was shown to be upregulated at 1.5 and 3 hours after exposure to Co (II) (Table A-1). To further explain the GABA shunt in *D. hansenii*, Figure 5-1, generated online via Interactive Pathways (Ipath) explorer v2 (Kanehisa et al., 2014; Ogata et al., 1999) shows the downregulated enzyme aconitase (aconitate hydratase, Table A-1). As can be seen in Figure 5-1, the TCA cycle cannot progress due to a lack of expression of an essential enzyme within the cycle. This enzyme does not significantly affect potential generation in the mitochondrial electron transport chain because NADH supply can be preserved by the GABA shunt (Tretter and Adam-Vizi, 2000).

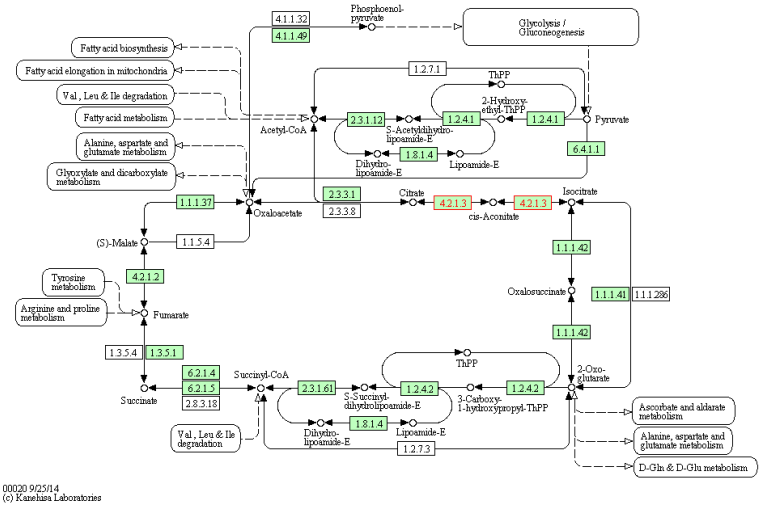

Figure 5-1: TCA cycle. Enzyme marked in red (cis-Aconitase) is shown to be downregulated in *D. hansenii* when exposed to 5mM Co (II). Downregulation or inhibition of cis-Aconitase blocks the TCA cycle, thus providing evidence of *D. hansenii's* use of the GABA shunt (Kaneshia et al., 2014; Ogata et al, 1999).

Succinate dehydrogenase, another TCA cycle and electron transport chain (complex II) enzyme, was also found to be inhibited by oxidative stress. Specifically, four different genes encoding succinate dehydrogenase subunits were significantly downregulated throughout all three time points; two were flavoprotein subunits, one was a cytochrome b subunit, and one was an iron-sulfur subunit (Table A-1). Superoxide production from the electron transport chain is achieved through electron leakage when these are being transported through the chain, localized to complex I and III (Lambert et al., 2004), and by complex I and II NADH dehydrogenase activity (Lambert et al., 2004). Within the electron carriers in complex I, flavin and iron-sulfur centers are found (Lambert et al., 2004). The downregulation of these four succinate dehydrogenase subunits suggests that the cells have decreased superoxide production by normal metabolic processes. This reduction prevents the coupling of metabolic superoxide production with superoxide production caused by exposure to heavy metals, and the subsequent increase in oxidative stress.

In response to oxidative stress caused by heavy metal exposure, *D. hansenii* showed downregulation of enzymes required for the elimination of toxic radical species (Table A-1). However, a non-enzymatic defense system is evidenced by the upregulation of glutatuione S-transferase 1, sulfiredoxin, lysine

and histidine metabolism, and sphingosine N-acyltranseferase LAG1 (Table A-1). Studies have shown that glutathione acts as a free radical scavenger (Jamieson et al., 1998) and sulfiredoxin acts as an antioxidant that may be involved in repair and signaling pathways of protein damage caused by oxidation (Biteau et al., 2003). Other important genes that were upregulated at the last two time points include genes for the biosynthesis of lysine and histidine which act in non-enzymatic oxidative stress response (Pearce et al., 1999); many of the genes upregulated in the transporter category were lysine and histidine specific as well. Histidine is believed to work against heavy metal toxicity, as *his-* strains have been found to be more sensitive to heavy metals such as copper, cobalt or nickel (Freire-Picos et al., 2006; Pearce et al., 1999). BUL1, needed for polyubiquitination and intracellular trafficking of GAP1 (Bach et al., 2009) was found to be upregulated at the first two time points, then downregulated at the 3 hour mark (Table A-1). Within the mechanisms for non-enzymatic oxidative stress response, protein STB5, highly upregulated at the 3-h time point, is known to be upregulated as a response to oxidative stress and is a known regulator of genes related to the pentose phosphate pathway and genes for the production of NADPH (Larochelle et al., 2006). The use of pentose phosphate pathway in non-enzymatic response to oxidative stress is due to the production of NADPH

which reduces oxidized glutathione, the free radical scavenger (Jamieson et al., 1998). Thus, STB5 activates the pentose phosphate pathway along with other genes for the production of NADPH as a response to oxidative stress. LAG1, which has a lipid metabolism function and is a ceramide synthesis component was also found to be upregulated in response to oxidative stress. Ceramides have been found to be induced under oxidative stress conditions (Van Brocklyn and Williams, 2012).

5.3 Cell Wall Integrity and Growth

Recovery from oxidative damage resulting from exposure to cobalt can be seen by the upregulation of genes for vegetative growth (Table A-1). Specifically, upregulation of paxillin-like protein 1 (PXL1, a Rho-family GTPase required for vegetative growth and mating) was observed at all three time points. PXL1 is a cell growth mediator that is necessary for selection and maintenance of polarized growth sites in the actin cytoskeleton (Mackin et al., 2004). Polarized cell growth is achieved through cascading events, where bud site selection occurs soon after localization of the signal (Mackin et al., 2004). These steps can progress through BUD4, which controls bud placement in haploid cells and was also found to be upregulated (Mackin et al, 2004). In this case, cell division seems to be achieved

through vegetative growth and not by sporulation, as seen by the downregulation of SEF1 (Table A-1). Other genes that contribute to cell division and growth found to be upregulated were a karyogamy protein (KAR4), a chromatin assembly gene (chromatin assembly factor 1 subunit p90), and RNA polymerase I. Also, within the carbohydrate metabolism category, GAS1 (1, 3-beta-glucanosyltransferase) was found to be upregulated the first 30 minutes after cobalt exposure. Upregulation of genes for cell wall components and cell parts throughout all three time points indicates that *D. hansenii* goes through recovery within the first three hours after exposure to subtoxic levels of cobalt (Table A-1).

CHAPTER 6 - CONCLUSION

D. hansenii is a highly extremophilic yeast. However, unlike in the case of osmotolerance (Arroyo Gonzalez et. al. 2009), resistance to concentrations of cobalt that are toxic to other similar organisms does not seem to be a pre-adapted characteristic. This is supported by the fact that there is an initial shock when *D. hansenni* is exposed to Co (II), as indicated by the observation that many of the genes that are upregulated several fold are involved in DNA synthesis and repair. Even though cells undergo shock, they respond rapidly to oxidative stress as a consequence of heavy metal exposure. Apart from activating mechanisms to eliminate free radical species non-enzymatically, *D. hansenii* also has the capability of averting natural metabolic processes that produce oxygen radicals. This response is so effective that an initial recovery of this organism is demonstrated by the upregulation of vegetative growth mechanisms as early as three hours after exposure. It would be interesting to monitor growth after the three hour time point in order to ascertain the time required for a complete recovery.

REFERENCES

André B. 1990. The UGA3 gene regulating the GABA catabolic pathway in Saccharomyces cerevisiae codes for a putative zinc-finger protein acting on RNA amount. *Mol. Gen. Genet.*, **220**: 269–76.

Arroyo Gonzalez N, Vazquez A, Ortiz Zuazaga HG, Sen A, Luna Olvera H, Peña de Ortiz S, N. S. G. 2009. Genome-wide expression profiling of the osmoadaptation response of Debaryomyces hansenii. *Yeast*, **26**: 111–124.

Auer PL, Doerge RW. 2010. Statistical design and analysis of RNA sequencing data. *Genetics*, **185**: 405–16.

Ashburner M, Ball CA, Blake JA, Botstein D, Butler H, Cherry JM, Davis AP, Dolinski K, Dwight SS, Eppig JT, Harris MA, Hill DP, Issel-Tarver L, Kasarskis A, Lewis S, Matese JC, Richardson JE, Ringwald M, Rubin GM, Sherlock G. Gene Ontology: tool for the unification of biology. *Nat Genet* 2000; **25**: 25-29.

Bach B, Meudec E, Lepoutre J-P, Rossignol T, Blondin B, Dequin S, Camarasa C. 2009. New insights into {gamma}-aminobutyric acid catabolism: Evidence for {gamma}-hydroxybutyric acid and polyhydroxybutyrate synthesis in Saccharomyces cerevisiae. *Appl. Environ. Microbiol.*, **75**: 4231–9.

Biteau B, Labarre J, Toledano MB. 2003. ATP-dependent reduction of cysteine-sulphinic acid by *S. cerevisiae* sulphiredoxin. *Nature*; **425**: 980-984.

Breuer U, Harms H. 2006. Debaryomyces hansenii--an extremophilic yeast with biotechnological potential. *Yeast*, **23**: 415–37.

Bullard JH, Purdom E, Hansen KD, Dudoit S. 2010. Evaluation of statistical methods for normalization and differential expression in mRNA-Seq experiments. *BMC Bioinformatics*, **11**: 94.

Chi Z-M, Liu G, Zhao S, Li J, Peng Y. 2010. Marine yeasts as biocontrol agents and producers of bio-products. *Appl. Microbiol. Biotechnol.*, **86**: 1227–41. http://www.ncbi.nlm.nih.gov/pubmed/20195858.

Coleman ST, Fang TK, Rovinsky S a, Turano FJ, Moye-Rowley WS. 2001. Expression of a glutamate decarboxylase homologue is required for normal oxidative stress tolerance in Saccharomyces cerevisiae. *J. Biol. Chem.*, **276**: 244–50.

Dallabona C, Marsano RM, Arzuffi P, Ghezzi D, Mancini P, Zeviani M, Ferrero I, Donnini C. 2010. Sym1, the yeast ortholog of the MPV17 human disease protein, is a stress-induced bioenergetic and morphogenetic mitochondrial modulator. *Hum. Mol. Genet.*, **19**: 1098–107.

Desnos-Ollivier M, Ragon M, Robert V, Raoux D, Gantier JC and Domer F. 2008. *Debaryomyces hansenii* (*Candida famata*), a rare human fungal pathogen often misidentified as *Pichia guilliermondii* (*Candida guilliermondii*). *J Clin Microbiol* **46**: 3237-3242

Dujon B, Sherman D, Fischer G et al. Genome evolution in yeasts. *Nature* 2004; **430**: 35-44.

Freire-Picos M a., Lamas-Maceiras M. 2006. KlHIS4-modulated histidine auxotrophy in yeast and characterisation of a KlHIS4-lacZ-based cadmium and copper biosensor. *Enzyme Microb. Technol.*, **40**: 67–70.

Gadd GM, Edwards SW. 1986. Heavy-metal induced flavin production in *Debaryomyces hansenii* and possible connections with iron metabolism. *Trans. Br. Mycol. Soc*. **87:** 533-542.

Gasch AP, Huang M, Metzner S, Botstein D, Elledge SJ, Brown PO. 2001. Genomic Expression Responses to DNA-damaging Agents and the Regulatory Role of the Yeast ATR Homolog Mec1p. *Mol. Biol. Cell*, **12**: 2987–3003.

Gault N, Sandre C, Poncy JL, Moulin C, Lefaix JL, Bresson C. 2010. Cobalt toxicity: Chemical and radiological combined effects on HaCaT keratinocyte cell line. *Toxicol. Vitr.*, **24**: 92–98.

Groom KR, Heyman HC, Steffen MC, Hawkins L, Martin NC. 1998. Kluyveromyces lactis SEF1 and its Saccharomyces cerevisiae Homologue

Bypass the Unknown Essential Function , but not the Mitochondrial RNase P Function , of the S . cerevisiae RPM2 Gene. *Yeast*, **87**: 77–87.

Horak CE, Luscombe NM, Qian J, Bertone P, Piccirrillo S, Gerstein M, Snyder M. 2002. Complex transcriptional circuitry at the G1/S transition in Saccharomyces cerevisiae. *Genes Dev.*, **16**: 3017–33.

Inglis DO, Arnaud MB, Binkley J, Shah P, Skrzypek MS, Wymore F, Binkley G, Miyasato SR, Simison M, Sherlock G. The *Candida* Genome Database incorporates multiple Candida species: multispecies search and analysis tools with curated gene and protein information for *Candida albicans* and *Candida glabrata*. *Nuc Acids Res* 2012; **40**: 6667-6674.

Jamieson DJ. 1998. Oxidative Stress Responses of the Yeast Saccharomyces cerevisiae. *Yeast*, **14**: 1511–1527.

Jeong H-S, Backlund PS, Chen H-C, Karavanov A a, Crouch RJ. 2004. RNase H2 of Saccharomyces cerevisiae is a complex of three proteins. *Nucleic Acids Res.*, **32**: 407–14.

Kanehisa M, Goto S, Sato Y, Kawashima M, Furumichi M, Tanabe M. 2014. Data, information, knowledge and principle: Back to metabolism in KEGG. *Nucleic Acids Res.*, **42**: 199–205.

Keeling PJ et al. 2014. The Marine Microbial Eukaryote Transcriptome Sequencing Project (MMETSP): Illuminating the Functional Diversity of Eukaryotic Life in the Oceans through Transcriptome Sequencing. **12**.

Kutty SN, Philip R. 2008. Marine yeasts — a review. 465–483.

Lambert AJ, Brand MD. 2004. Inhibitors of the quinone-binding site allow rapid superoxide production from mitochondrial NADH:ubiquinone oxidoreductase (complex I). *J. Biol. Chem.*, **279**: 39414–20.

Larochelle M, Drouin S, Robert F, Turcotte B. 2006. Oxidative stress-activated zinc cluster protein Stb5 has dual activator/repressor functions required for pentose phosphate pathway regulation and NADPH production. *Mol. Cell. Biol.*, **26**: 6690–701.

Lewis M, Pryor R, Wilking L. 2011. Fate and effects of anthropogenic chemicals in mangrove ecosystems: A review. *Environ. Pollut.*, **159**: 2328–2346..

Li A, van Luijk N, ter Beek M, Caspers M, Punt P, van der Werf M. 2011. A clone-based transcriptomics approach for the identification of genes relevant for itaconic acid production in Aspergillus. *Fungal Genet. Biol.*, **48**: 602–11.

Mackin NA, Sousou TJ, Erdman SE. 2004. The PXL1 Gene of Saccharomyces cerevisiae Encodes a Paxillin-like Protein Functioning in Polarized Cell Growth. *Mol. Biol. Cell*, **15**: 1904–1917.

Marioni JC, Mason CE, Mane SM, Stephens M, Gilad Y. 2008. RNA-seq: an assessment of technical reproducibility and comparison with gene expression arrays. *Genome Res.*, **18**: 1509–17.

Marks VD, Ho Sui SJ, Erasmus D, van der Merwe GK, Brumm J, Wasserman WW, Bryan J, van Vuuren HJJ. 2008. Dynamics of the yeast transcriptome during wine fermentation reveals a novel fermentation stress response. *FEMS Yeast Res.*, **8**: 35–52.

Michaeli S et al. 2011. A mitochondrial GABA permease connects the GABA shunt and the TCA cycle, and is essential for normal carbon metabolism. *Plant J.*, **67**: 485–98.

Nies, DH. Microbial heavy-metal resistance. *Appl Microbiol Biotechnol*. 1999; **51**: 730–750.

Ogata H, Goto S, Sato K, Fujibuchi W, Bono H, Kanehisa M. 1999. KEGG: Kyoto encyclopedia of genes and genomes. *Nucleic Acids Res.*, **27**: 29–34.

Pearce DA, Sherman F. 1999. Toxicity of Copper , Cobalt , and Nickel Salts Is Dependent on Histidine Metabolism in the Yeast Saccharomyces cerevisiae. *J. Bacteriol*, **181**: 4774–4779.

Prista C, Almagro A, Ramos J, Prista C, Almagro A, Loureiro-dias MC, Microbiologı D De. 1997. Physiological basis for the high salt tolerance of Debaryomyces hansenii . Physiological Basis for the High Salt Tolerance of Debaryomyces hansenii. **63**.

Rainbow PS. 1995. Biomonitoring of Heavy Metal Availability in the Marine Environment. *Mar. Pollut. Bull.*, **31**: 183–192.

Seda-Miró JM, Arroyo-González N, Pérez-Matos A, Govind NS. 2007. Impairment of cobalt-induced riboflavin biosynthesis in a Debaryomyces hansenii mutant. *Can. J. Microbiol.*, **53**: 1272–7.

Sulahian R, Sikder D, Johnston SA, Kodadek T. 2006. The proteasomal ATPase complex is required for stress-induced transcription in yeast. *Nucleic Acids Res.*, **34**: 1351–7.

Tretter L, Adam-vizi V. 2000. Inhibition of Krebs Cycle Enzymes by Hydrogen Peroxide : A Key Role of alpha-Ketoglutarate Dehydrogenase in Limiting NADH Production under Oxidative Stress. *J. Neurosci.*, **20**: 8972–8979.

Valko M, Morris H, Cronin MTD. 2005. Metals, toxicity and oxidative stress. *Curr. Med. Chem.*, **12**: 1161–208.

Van Brocklyn JR, Williams JB. 2012. The control of the balance between ceramide and sphingosine-1-phosphate by sphingosine kinase: oxidative stress and the seesaw of cell survival and death. *Comp. Biochem. Physiol. Part B*, **163**: 26–36.

Wolf JBW. 2013. Principles of transcriptome analysis and gene expression quantification: an RNA-seq tutorial. *Mol. Ecol. Resour.*, **13**: 559–72.

APENDIX

Table A-1: Genes, GO process annotation, fold change, and temporal clustering of the 471 genes that demonstrated a four-fold change or more at any time point after exposure to cobalt.

Cluster	Clustering similarity	Gene	Similarity to Gene	GO Term	Gene Function	Fold Change of Differentially Expressed Genes (log_2)		
						0.5-h	1.5-h	3-h
5	0.924042846	DEHA2A06820g	H	ion binding	Subunit NUHM of protein NADH:Ubiquinone Oxidoreductase (Complex I)	0.71776698	**2.02597039**	**2.29883449**
1	0.898006577	DEHA2G24266g		molecular function		**4.345676632**	**3.547928694**	**4.908670403**
1	0.924771573	DEHA2A06292g		amino acid metabolism	Ornithine carbamoyltransferase	1.419368209	0.851386429	**2.336090092**
5	0.878727236	DEHA2A06710g		binding	Iron assembly protein 1	-1.35372903	**-2.36521063**	-1.74026817
5	0.976549806	DEHA2A01980g	W	molecular function		-1.6997392	**-3.00179372**	**-3.40599002**
2	0.99529314	DEHA2A03806g	W	unknown		-1.40661557	0.254895968	0.65500347
5	0.872059286	DEHA2A08052g		biological process		**-2.11855244**	-1.08690621	**-2.75131457**

2	0.88479957	DEHA2A02398g		molecular function		**-2.07072083**	-1.14391024	0.233267641
1	0.988460915	DEHA2A13354g		unknown		1.239977486	1.936973379	**2.593711928**
2	0.968740695	DEHA2A00770g		molecular function		**-2.75766317**	0.817558953	0.805046529
6	0.893734906	DEHA2A12254g		unknown		-0.25151642	0.539576598	-1.49799667
1	0.979048485	DEHA2A10802g	W	binding	Calcium-binding mitochondrial carrier SAL1	1.027707439	0.95022259	**2.095981513**
5	0.841575885	DEHA2A09570g		binding	Exosome complex component CSL4	-1.01719118	**-2.11762156**	-1.44011458
5	0.704240013	DEHA2A13882g		carbohydrate metabolism	Alpha-glucosidase MAL12	**-2.08903245**	-0.33143141	**-2.54369845**
6	0.975807742	DEHA2A09350g		transporter activity	ADP-ribosylation factor 3	0.2565758	-0.87883275	**-3.50641295**
2	0.732437086	DEHA2A12562g		unknown	SUMO-conjugating enzyme UBC9	**-2.27233252**	0.231293804	-0.94693366
6	0.942933006	DEHA2A11352g	H	ion binding	SUMO-conjugating enzyme UBC9	-0.52988825	-0.76613565	**-2.22730337**
2	0.994668722	DEHA2A06754g	W	transporter activity	Pleiotropic drug resistance regulatory protein	**-2.21028657**	-0.24007515	0.722103049

3	0.913305381	DEHA2A02090g		amino acid metabolism	Catabolic L-seriene/threonine dehydratse	-1.08989999	**-2.47711603**	0.196544163
5	0.980932669	DEHA2A09086g		transporter activity	Calcium-transporting ATPase 2	-1.88981758	-1.78236359	**-2.46283431**
5	0.956867374	DEHA2A01056g	W	molecular function		**-2.45378821**	-1.91789966	**-3.34321086**
3	0.953066038	DEHA2A11132g	W	unknown		0.690338869	-1.88239212	0.431725775
1	0.863979768	DEHA2A01694g		molecular function		-0.13232993	1.546693606	**2.669761974**
2	0.758945533	DEHA2A03564g		unknown		**-2.02194279**	-1.10008974	-0.7527886
1	0.921124529	DEHA2A12606g		binding	Structural maintenance of chromosomes protein 5	0.293481036	0.766857193	**2.16258758**
3	0.850630451	DEHA2A05214g	W	unknown		0.09744834	-0.75520611	1.564222096
5	0.947968422	DEHA2A07942g		protein metabolism	Ubiquitin carboxyl-terminal hydrolase 3	-0.9731521	-1.06583546	**-2.22149589**
5	0.635650383	DEHA2A00902g		transferase activity	Ribosomal RNA methyltransferase MRM2, mitochondrial	**-2.65493915**	-0.94523371	-1.73977896
5	0.94099169	DEHA2A11440g		transporter activity	Synchronized import protein 1	-0.61930165	-1.1777877	**-2.00108843**

4	0.948443847	DEHA2C16698g		ion binding	DNA repair protein RAD51	**4.321456813**	**3.946156954**	**3.670005253**
3	0.959646868	DEHA2A02134g		unknown		0.514807958	-1.10827625	1.266086955
6	0.986195771	DEHA2A05808g		binding	DNA replication complex GINS protein PSF3	0.606562729	0.081449313	**-2.06590503**
4	0.81146242	DEHA2E18876g		physiological response to stimulus	Cellular response to drug/ Possible protease	**3.956330756**	1.406714813	**3.63422615**
2	0.928430827	DEHA2A06094g	W	unknown		-1.9787246	0.750275551	0.344143605
2	0.917309254	DEHA2A01738g		unknown		-1.17110958	-0.25478519	1.121585104
4	0.907580092	DEHA2C00484g		unknown		**3.83333803**	**3.917457352**	**3.676839944**
5	0.743381459	DEHA2A06688g		unknown		-1.38029655	**-2.15108889**	-1.14347724
3	0.987084239	DEHA2A08558g		unknown		-0.17383128	**-2.99009902**	0.382599426
2	0.962795135	DEHA2A07568g		unknown		-1.76814133	-0.54343212	0.54806437
2	0.908632469	DEHA2A01408g	H	unknown		-0.76521186	0.62851016	1.48112808
4	0.960760206	DEHA2C00836g	W	amino acid	Transcriptional activator protein UGA3	**3.504505678**	**3.301262682**	**2.636785275**

				metabolism				
6	0.855360816	DEHA2B14652g	W	unknown		-0.34519998	0.785868832	-1.70554897
2	0.709329051	DEHA2B00110g		unknown		**-3.11237628**	**-2.32351028**	-0.90946252
1	0.898510677	DEHA2B01496g		catalytic activity	ATPase synthesis protein 25, mitochondrial	0.157639741	0.6904719	**2.098685804**
4	0.962341675	DEHA2B15818g		ion binding	DNA mismatch repair protein MSH2	**3.367497785**	**2.419017479**	**2.73534866**
5	0.967724714	DEHA2B06974g	W	ion binding	Brown 2	-1.00774779	-1.91511854	**-2.12403992**
1	0.973546076	DEHA2B12342g	H	molecular function		1.408388126	1.406723507	**2.102216251**
2	0.923051502	DEHA2B11352g		unknown		-0.85353736	0.786725588	1.352434317
4	0.972464153	DEHA2E04862g	W	ion binding	Paxillin-like protein 1	**3.134800395**	**2.659211329**	**2.39841948**
3	0.892896979	DEHA2B04774g	W	protein metabolism	Protein N-terminal amidase	-0.81267266	**-2.19183647**	-0.35176203
5	0.860781614	DEHA2B13926g		molecular function		**-2.18996748**	-1.40556951	-1.99369471
4	0.846105839	DEHA2B16258g		catalytic activity	Alpha-L-arabinofuranosidase, putative	1.688854928	**2.202095934**	1.648799634

5	0.926370168	DEHA2B13398g	H	binding	Multifunctional methyltransferase subunit TRM112	-1.06204709	-0.91100579	**-2.2075846**
5	0.832050241	DEHA2B16192g		unknown		**-3.09062293**	**-2.77642519**	**-2.39926979**
1	0.975512691	DEHA2B14740g		transporter activity	Polyamine transporter 3	0.756878612	1.48650148	**2.815337942**
5	0.970924503	DEHA2B13706g		transporter activity	Protein CCC1	**-2.80549765**	**-3.26148122**	**-3.43747535**
2	0.838575873	DEHA2B16038g		unknown		-0.57953262	0.318864031	1.683126534
2	0.99285761	DEHA2B15400g	W	unknown		-1.45891955	0.324969575	0.743604811
1	0.914821005	DEHA2B14696g		molecular function		1.389695579	**3.748123158**	**3.913754694**
2	0.936944637	DEHA2B12320g		unknown		-1.29405202	0.823564297	1.879343591
1	0.864208624	DEHA2B15576g	W	carbohydrate metabolism	6-phosphofructo-2-kinase 2	1.732731861	**2.158493937**	**2.000478767**
1	0.946861938	DEHA2B08184g		ion binding	Mitochondrial nuclease	1.381525014	1.867745389	**2.073947357**
6	0.950544773	DEHA2B03014g		amino acid metabolism	Aspartate aminotransferase, cytoplasmic	-0.38904563	-0.7406678	**-2.12394417**

1	0.993878295	DEHA2B14476g		molecular function		0.846124492	1.086692142	**2.085338488**
1	0.985686808	DEHA2B16346g		unknown		1.561548283	1.502349373	**2.722959163**
1	0.921083257	DEHA2G21780g		molecular function		**2.938856704**	**2.227560731**	**3.6568597**
5	0.88871567	DEHA2B04752g	W	carbohydrate metabolism	Protein MNN4	-1.1356929	-0.8183197	**-2.46107827**
5	0.888901674	DEHA2B05632g	W	binding	Kinetochore-associated protein MTW1	-0.62540672	-1.71684769	**-3.28933869**
2	0.99955355	DEHA2B10120g		lipid metabolism	Long-chain-fatty-acid--CoA ligase	**-2.13077635**	-0.02055177	0.696356141
5	0.960540918	DEHA2B16170g	W	transporter activity	Zinc-regulated transporter	**-2.35540346**	**-2.11962057**	**-2.70124974**
5	0.966349813	DEHA2B16126g		carbohydrate metabolism	Alpha-glucosidase	**-2.34004748**	**-2.27453709**	**-2.71365994**
5	0.922421743	DEHA2B05522g		transporter activity	Mitochondrial carnitine carrier	-0.68880741	-1.73007963	**-2.75418705**
3	0.812329008	DEHA2B10934g	W	unknown		-0.20983443	-0.95610921	1.848475647
5	0.833963377	DEHA2B04532g	W	ion binding	Phosphatidylinositol-3-phosphate-binding protein 2	-0.14426476	-1.91071522	**-2.82151345**

2	0.717375264	DEHA2B16060g	molecular function	5-aminolevulinate synthase, mitochondrial	**-2.62585835**	-1.86717575	-0.82673038
1	0.990109886	DEHA2B09482g	molecular function		1.054876853	1.364268991	**2.738515081**
5	0.944432628	DEHA2B05478g	ion binding	5-aminolevulinate synthase, mitochondrial	-0.96823133	-1.93513878	**-3.10684779**
5	0.923106762	DEHA2B04488g	oxidation-reduction process	Mitochondrial inner membrane protein SHH3	-1.79104739	**-3.0006312**	**-2.50895689**
6	0.973410318	DEHA2B09966g	unknown		0.579528776	0.034683057	-1.51660613
1	0.913044662	DEHA2D16280g	amino acid metabolism	Glutathione S-transferase 1	**2.89016516**	**3.678978999**	**3.783618496**
6	0.827187813	DEHA2B08008g	unknown		1.491040147	0.885437667	-0.8692844
2	0.804576529	DEHA2B06996g	cell part	Protein ILM1	**-3.09994518**	-1.68742308	-0.86561862
2	0.923738294	DEHA2B01826g	molecular function		**-2.53313488**	-0.1698048	-0.32628206
5	0.998895821	DEHA2B16104g	transporter activity	Maltose permease MAL31; Maltose permiase MAL61	**-2.33315638**	**-2.6954802**	**-3.5825784**
3	0.826722906	DEHA2B09636g	binding	Vacuolar protein sorting-associated protein 28	0.16504138	**-2.00558491**	-0.5808325
2	0.900284034	DEHA2B12254g	unknown		-1.63429375	-0.82509162	0.589983742

3	0.881300879	DEHA2B08690g		unknown		1.033354937	-0.65438814	1.665885602
3	0.851696965	DEHA2B01606g		unknown		0.849496659	-1.15634251	0.201279434
2	0.897389291	DEHA2B15004g	W	binding		-1.08805208	0.494430142	**2.093905919**
5	0.977215353	DEHA2B04796g	W	protein metabolism	Protein MNN4	-1.14382782	-1.22438145	**-2.17390401**
4	0.968043978	DEHA2C05720g		amino acid metabolism	Acetylornithine aminotransferase, mitochondrial	**2.890144909**	1.519902968	1.900687972
1	0.85803737	DEHA2B02420g	H	amino acid metabolism	Argininosuccinate synthase	1.47054328	0.57138692	**2.22919618**
1	0.985670322	DEHA2B11968g	W	transporter activity	Phosphatidylinositol transfer protein SFH5	1.049075496	**2.015630103**	**3.092032823**
3	0.868756732	DEHA2B10978g		unknown		-0.38267047	-1.15177444	1.234354997
6	0.746172678	DEHA2C04444g		unknown		-0.02838671	1.327243844	-1.17516845
2	0.773125454	DEHA2C06314g		oxidation-reduction process	Ferric reductase transmembrane component 4	-1.11282157	**2.037221433**	1.05963021
5	0.856957096	DEHA2C11660g	H	amino acid	3-isopropylmalate dehydratase	-1.39718715	**-3.70668239**	**-2.81106285**

				metabolism				
3	0.970396728	DEHA2C10626g		unknown		-0.31120971	-1.49747025	0.617014796
4	0.933878334	DEHA2G13310g		ion binding	Dephospho-CoA kinase CAB5	**2.821370391**	**2.11054079**	**2.556339098**
6	0.975858427	DEHA2C04224g	W	catalytic activity	SAGA-associated factor 73	-0.51578194	-0.57233126	**-2.88243055**
4	0.831382453	DEHA2C16676g		ion binding	Putative transcription factor SEF1	1.55606503	**2.154797195**	1.406478454
2	0.74739134	DEHA2C13200g		molecular function		**-2.21100897**	-0.67264287	-1.0185504
3	0.778467579	DEHA2C01144g		molecular function	Cobalamin synthesis protein, putative	-0.86313299	**-2.04090868**	-0.78529484
3	0.790354634	DEHA2C04752g	W	transferase activity	Serine/threonine-protein kinase TEL1	-0.11856829	**-2.01603217**	-0.78040477
3	0.985055967	DEHA2C16170g		binding	Nucleolar protein 12	0.773309199	**-2.07951868**	1.439766382
6	0.911336665	DEHA2C15136g		molecular function		-0.89029095	-0.86831258	**-2.5237131**
1	0.918045065	DEHA2C17006g		cell part/ cell assembly	Ortholog of *S. cerevisiae* Gpa15	1.909917044	1.154002197	**2.802272809**
3	0.83791924	DEHA2C04532g		oxidation-reduction process	NADPH dehydrogenase 2	0.993989421	-0.67617902	**2.55317764**

3	0.983257333	DEHA2C00748g	W	unknown		0.128061794	-1.87273316	0.258966324
6	0.921639894	DEHA2C16016g		unknown		-0.42108525	0.366974456	-1.94769718
3	0.68679485	DEHA2C01672g	W	unknown		-0.71783296	-0.85122507	1.969075252
1	0.95200337	DEHA2C00682g		catalytic activity	L-2,3-butanediol dehydrogenase/acetoin reductase	0.799509333	**2.54342389**	**4.189191258**
1	0.821596371	DEHA2C14894g		catalytic activity	CoA-transferase family protein	1.00899167	**2.01825098**	1.566937612
6	0.879939432	DEHA2C08448g		unknown		0.25019945	-0.95761963	-1.88876093
6	0.951941839	DEHA2C03960g		binding		0.22191727	-0.72086199	**-2.18913793**
1	0.993518319	DEHA2C05830g		molecular function		1.268609919	1.409918637	**2.719754662**
1	0.993124319	DEHA2C06248g	W	oxidation-reduction process	Ferric reductase transmembrane component 4	1.498272325	**2.421825812**	**3.488670541**
6	0.85731174	DEHA2C09966g		unknown		0.921250805	1.173854234	-1.01619178
1	0.929483703	DEHA2C03388g		molecular function		0.524035307	**2.053478994**	**2.717550011**
4	0.826740969	DEHA2D14982g		ion binding	Deoxyuridine 5'-triphosphate nucleotidohydrolase	**2.703992506**	1.930234362	0.012195875

1	0.802711335	DEHA2C08052g		unknown		0.137262059	0.099301311	**2.29416642**
1	0.837856302	DEHA2C01012g		catalytic activity	Acid phosphatase	0.167857677	**3.724170848**	**4.079525413**
4	0.999252502	DEHA2E15466g	W	unknown		**2.688348971**	1.942216838	1.555249349
6	0.968704287	DEHA2C14344g		binding		0.010074341	-0.67010322	**-2.22865641**
6	0.966422127	DEHA2C03278g		unknown		0.696553196	0.57781316	-1.74492196
1	0.980542775	DEHA2C07018g	H	amino acid metabolism	Saccharopine dehydrogenase [NAD+, L-lysine-forming]	1.296820335	1.488522825	**2.052860965**
1	0.870529414	DEHA2C02288g		catalytic activity	NAD(P)H-hydrate epimerase	-0.08729818	0.962225118	**2.147528419**
1	0.887443669	DEHA2C06028g	W	protein metabolism	Ubiquitin-like-specific protease 2	1.548965325	0.842869075	**2.044851095**
4	0.978317343	DEHA2D16500g		catalytic activity	MutT/Nudix family hydrolase	**2.624576217**	**2.226222216**	1.34250946
3	0.679806673	DEHA2C17908g	W	catalytic activity	Unsaturated glucuronylhydrolase	-0.46032113	-0.68488381	**2.449429988**
1	0.96623613	DEHA2C15004g	H	amino acid metabolism	Imidazoleglycerol-phosphate dehydratase	1.634377528	1.678393899	**2.343509343**

1	0.973440573	DEHA2C16852g		amino acid metabolism	Homoisocitrate dehydrogenase, mitochondrial	1.823597507	**2.128002597**	**2.793853517**
1	0.841404554	DEHA2C00616g		unknown		1.708950268	0.555382027	**2.696746668**
3	0.750652909	DEHA2C01430g	W	carbohydrate metabolism	Probable family 17 glucosidase SCW4	0.558548276	**-2.06370649**	-0.71563582
5	0.948486014	DEHA2C12848g	H	transferase activity	Cytochrome C	-0.90902712	**-2.07864695**	**-2.36603231**
3	0.956435771	DEHA2C06446g		molecular function		-0.90821166	**-3.09529654**	1.018283014
2	0.907129849	DEHA2C11858g		unknown		-1.16594684	-0.05171603	1.522027486
1	0.867044916	DEHA2C13728g	H	amino acid metabolism	Histidinol-phosphatase	1.443651717	**2.340770318**	**2.031927669**
1	0.905673019	DEHA2C14652g		unknown		0.740170476	0.509004645	**2.29104069**
1	0.96904774	DEHA2C14608g		cell part/ cell assembly	SPS-sensor component PTR3	1.812313344	1.483341149	**3.192800592**
1	0.980696077	DEHA2C08250g		unknown		1.617854195	1.495098126	**2.699102032**

1	0.988872853	DEHA2C17402g		catalytic activity	Putative uncharacterized protein CaJ7.0344	0.735375279	1.302387297	**2.189086844**
1	0.878282769	DEHA2C06336g		transporter activity	Iron transporter FTH1	1.088351969	**2.060255146**	1.821987089
1	0.970474437	DEHA2C06270g		oxidation-reduction process	Sulfiredoxin	0.914854279	1.900141189	**2.433993939**
6	0.96656608	DEHA2C05280g		unknown		-0.33192991	-0.67679743	**-2.27214242**
4	0.812882953	DEHA2E16060g	W	binding	Chromatin assembly factor 1 subunit p90	**2.555121441**	**3.476521274**	1.228199693
4	0.983256965	DEHA2G04268g		oxidation-reduction process	Ribonucleoside-diphosphate reductase smallchain 1	**2.551583404**	**2.155060184**	1.753369934
1	0.94590206	DEHA2E18634g		catalytic activity	Cytochrome P450 52A12	**2.504412222**	**2.759252214**	**3.364614136**
1	0.887423643	DEHA2C17578g		molecular function		0.317220527	**2.202473556**	**2.661401074**
1	0.951055376	DEHA2C13332g		unknown		0.36828589	0.97510634	**2.01922772**
6	0.968601318	DEHA2C17468g	W	transporter activity	Chitin biosynthesis protein CHS6	0.134571069	-0.59494598	**-2.09326046**
1	0.893497762	DEHA2C04994g		unknown		1.881987828	1.242293423	**2.238685943**
6	0.877338159	DEHA2C04026g	W	unknown		0.286018733	-1.00547377	-1.97524535

5	0.918803413	DEHA2C03036g		oxidation-reduction process	Alpha-ketoglutarate-dependent sulfonate dioxygenase	-0.51433525	-1.47990054	**-2.13330342**
1	0.95056647	DEHA2E13970g	W	binding	Protein PLM2	**2.4222916**	**2.698864724**	**3.319784948**
2	0.879556682	DEHA2C14850g		unknown		-0.58838426	0.748233176	1.513736147
1	0.924774531	DEHA2F06930g		carbohydrate metabolism	D-lactate dehydrogenase [cytochrome] 1, mitochondrial	**2.408389853**	**2.566029594**	**2.999087324**
1	0.890385116	DEHA2B08954g		biological process	Ribosome assembly protein 3	**2.395668321**	**2.245527124**	**2.65191542**
6	0.963882809	DEHA2C17138g		unknown		0.504697479	0.714729633	-1.95789762
4	0.961342905	DEHA2A03498g		cell part	Covalently-linked cell wall protein 12	**2.39507008**	1.5799313	0.76725549
6	0.975534957	DEHA2C16148g		unknown		0.64207299	-0.03843329	-1.86547947
1	0.765311812	DEHA2C12298g		transporter activity	Kinesin-like protein KIP2	1.772081984	0.375362658	**2.284795058**
6	0.850757489	DEHA2C14168g		unknown		1.503527775	0.449235269	-1.1443249
6	0.963775263	DEHA2D09174g		unknown		-0.02110914	-0.76062738	**-2.36567056**
6	0.91176148	DEHA2D17380g		catalytic activity	Rhomboid protein 1, mitochondrial	-0.43726562	-1.33688866	**-2.83912048**

6	0.951060483	DEHA2D08184g		unknown		0.100774691	0.527688836	-1.51954696
5	0.945841583	DEHA2D02948g	H	ion binding	Subunit NUIM of protein NADH:Ubiquinone Oxidoreductase (Complex I)	-0.88803031	**-2.02055056**	**-2.817216**
6	0.934593887	DEHA2D01958g		unknown		0.715772213	-0.15034485	-1.42279435
4	0.961067899	DEHA2D09020g	W	protein metabolism	Ubiquitin ligase-binding protein BUL2	**2.389226721**	**2.303659034**	1.528260177
5	0.940403907	DEHA2D18106g		unknown		**-7.35424861**	**-7.51633785**	**-7.71843493**
5	0.89977966	DEHA2D10120g		amino acid metabolism	Transaminated amino acid decarboxylase	-1.31899838	-1.03569404	**-2.91321611**
6	0.936359644	DEHA2D16170g	W	unknown		0.792990408	0.089809118	-1.27049391
6	0.999625591	DEHA2D09548g		molecular function		0.269491413	-0.09821657	**-2.96644517**
2	0.860095346	DEHA2D01518g		oxidation-reduction process	Uncharacterized protein YKL070W	-0.81669109	1.547173037	**2.377775464**
6	0.950825609	DEHA2D11176g		unknown		0.459758101	-0.36818957	-1.61112259
6	0.911619113	DEHA2D17644g		unknown		1.030863422	0.861012746	-1.28159931

3	0.765807519	DEHA2D00462g		unknown		1.853961353	-0.31353021	1.78953507
5	0.629181725	DEHA2D01342g	W	protein metabolism	Thiol-specific monooxygenase	**-2.65800807**	-0.15499427	**-2.85367456**
2	0.830136652	DEHA2D07392g		molecular function		**-2.32708749**	0.714050183	-0.36056133
6	0.887458173	DEHA2D01232g		transporter activity	Fluconazole resistance protein 1	-0.99424695	0.053455289	**-2.55775434**
5	0.900569567	DEHA2D09152g		transporter activity	Putative mitochondrial carnitine O-acetyltransferase	-1.01991952	-0.82500326	**-2.30366481**
5	0.984133563	DEHA2D02970g		transporter activity	Carrier protein YMC1, mitochondrial	-1.21362689	-1.40451467	**-2.34374016**
5	0.708455983	DEHA2D02398g		cell part	Smr domain-containing protein YPL199C	-0.56657785	**-2.28626546**	-1.23816151
4	0.991180847	DEHA2F25344g		unknown		**2.384287667**	1.802393792	1.17909219
4	0.647738887	DEHA2D16038g	W	transporter activity	Hexose transporter HXT14	**2.375547933**	-0.38603022	0.605083821
6	0.921210051	DEHA2D18942g	W	transporter activity	Sugar transporter STL1	-0.59879552	-1.43445267	**-3.25382587**
5	0.938951861	DEHA2D15114g		transferase activity	tRNA (uracil-5-)-methyltransferase	-1.89250901	**-2.09139552**	**-2.020753**
5	0.975714256	DEHA2D14124g		amino acid metabolism	Dihydroxy-acid dehydratase, mitochondrial	-1.13844641	**-2.01897576**	**-2.27504032**

6	0.790596411	DEHA2D01650g		unknown		1.574858542	1.560641814	-0.82927612
1	0.97577817	DEHA2E13464g		unknown		**2.363002672**	**2.285784904**	**3.605048741**
4	0.876310272	DEHA2B00990g		unknown		**2.322139413**	**2.392170487**	**2.471892485**
1	0.816875355	DEHA2D11154g		molecular function		1.312096061	0.31059265	**2.16541214**
6	0.881167084	DEHA2D13838g		unknown		1.314250402	0.510467759	-1.17508901
3	0.925879369	DEHA2D16632g		unknown		0.752196554	-0.80018733	1.30311086
1	0.911582974	DEHA2D13772g		amino acid metabolism	ATP phosphoribosyltransferase	1.230836634	**2.163789383**	**2.087999736**
2	0.856144222	DEHA2D04356g	H	molecular function		**-2.14841969**	-1.33990485	0.324060517
4	0.91255655	DEHA2D09790g		lipid metabolism	C-8 sterol isomerase	**2.314858013**	**2.372718482**	**2.169937709**
6	0.718955409	DEHA2D01496g		unknown		-0.6371606	0.863811173	-1.40375137
5	0.874857318	DEHA2D15312g		unknown		-0.32582356	-1.28384183	**-2.25499308**
4	0.862973861	DEHA2C11572g	W	cell part	Nucleoporin NUP60	**2.30816681**	0.557351098	1.309723956

6	0.548813944	DEHA2D03256g	W	unknown		-1.27384637	0.690086413	-1.45148818
1	0.983935072	DEHA2D01276g	W	catalytic activity	Uncharacterized protein YLL056C	1.261274	**2.28893306**	**3.10141179**
6	0.962779263	DEHA2D09196g	W	unknown		0.983174075	0.276712136	-1.98707522
3	0.777174328	DEHA2D14102g		unknown		0.987184328	-0.17760226	1.86443773
6	0.987799962	DEHA2D09086g	W	protein metabolism	Ubiquitin ligase-binding protein BUL2	0.048825919	-0.50351394	**-2.45091611**
6	0.99094987	DEHA2D03894g		unknown		0.181760284	0.275761182	**-2.19382502**
4	0.926984309	DEHA2F21406g		binding	RNA polymerase I upstream control element sequence-specific DNA binding	**2.294435542**	**2.459022608**	1.829426825
5	0.984033746	DEHA2D18128g		unknown		**-2.22116038**	**-2.37537052**	**-2.84672415**
6	0.940440584	DEHA2D11990g		oxidation-reduction process	Cytochrome b-c1 complex subunit 6	-0.13822672	-0.879995	**-2.19487782**
1	0.995677747	DEHA2D10956g		unknown		1.649903082	1.89756637	**3.545820005**
1	0.951454275	DEHA2D04554g		transporter activity	Plasma membrane iron permease	1.031004383	**2.149204323**	**2.444437273**
6	0.8244342	DEHA2D12760g		unknown		1.198642883	0.143043826	-0.90517359

5	0.739996363	DEHA2D14168g		unknown		**-3.14540316**	-1.5893856	**-2.29475346**
4	0.908999179	DEHA2F15642g		transporter activity	Quinidine resistance protein 3	**2.289436979**	0.903033588	1.605533458
3	0.822112774	DEHA2D07634g		molecular function		**2.250874548**	-0.67985939	**2.663455469**
2	0.647925392	DEHA2D15510g	W	unknown		-0.87469458	1.202665963	0.042356849
5	0.964702773	DEHA2D16896g	W	ion binding	ATP-dependent DNA helicase MPH1	-1.31411016	-1.53900233	**-2.88724871**
6	0.779093992	DEHA2D01584g		unknown		0.914851004	1.370718606	-0.7057665
1	0.99479796	DEHA2D10626g		cell part/ cell assembly	Nitrosoguanidine resistance protein SNG1	1.27881218	1.519411625	**2.904113339**
6	0.889081812	DEHA2D18590g		unknown		-0.19630908	0.61679398	-1.47594186
6	0.945926309	DEHA2D02354g	W	binding	DNA replication regulator DPB11	-0.1579322	0.720135965	**-2.67233693**
6	0.933812716	DEHA2D18546g		ion binding	tRNA modification GTPase MSS1, mitochondrial	-0.86782575	-0.68780394	**-2.68478863**
5	0.747766668	DEHA2D18480g		transferase activity	3-ketoacyl-CoA thiolase, peroxisomal	**-2.59940649**	-0.9521566	**-2.344719**
3	0.923014697	DEHA2E09152g	W	unknown		0.529529363	-1.11322186	1.781573364

4	0.896786203	DEHA2C11528g		carbohydrate metabolism	1,3-beta-glucanosyltransferase GAS1	**2.23877475**	1.433708497	0.325728556
3	0.979885258	DEHA2E03806g		unknown		0.464890165	-1.80193114	0.502650056
4	0.876659543	DEHA2D07040g	H	amino acid metabolism	Urea amidolyase	**2.224139946**	0.704220597	0.448467133
1	0.941057908	DEHA2E21626g	H	binding	Transcriptional activator HAP3	0.476266814	1.834382547	**3.073767928**
5	0.984891348	DEHA2E02288g	W	binding	Sequence-specific DNA binding transcription factor activity	**-2.51542861**	**-2.96591346**	**-3.3319399**
6	0.99523517	DEHA2E01298g		unknown		-0.09761135	-0.3014728	**-2.31292378**
6	0.744933356	DEHA2E13244g		unknown		-0.73222334	0.738480008	-1.56321089
5	0.999582513	DEHA2E03058g	W	transporter activity	Transport protein particle 130 kDa subunit	-1.75867769	**-2.16766605**	**-2.7851118**
1	0.976210261	DEHA2E01078g		catalytic activity	Putative uncharacterized protein B11H24.110	1.04166466	**2.246237464**	**3.813171832**
5	0.530271358	DEHA2E17732g	W	molecular function		**-2.00978572**	0.051813039	-1.75529212
1	0.973671583	DEHA2E04686g	W	cell part/ cell assembly	Uncharacterized protein YLR287C	1.059350476	0.970216398	**2.302501031**

2	0.894207013	DEHA2E22110g		unknown		-0.67603355	0.680619405	1.507427794
1	0.765521697	DEHA2E07480g	W	ion binding	Protein STB5	1.600873781	0.082014022	**2.851686024**
3	0.825051975	DEHA2E18502g		unknown		1.180234511	-0.38126985	1.836131473
1	0.996650297	DEHA2E09306g	W	unknown		1.566804639	**2.433089301**	**3.775297343**
1	0.964178611	DEHA2E02596g	W	transporter activity	Siderophore iron transporter 1	0.659016219	1.704599855	**2.474495158**
3	0.837055484	DEHA2E13618g		unknown		0.712101644	-0.55108325	**2.011012261**
3	0.916190952	DEHA2E12628g		unknown		-0.75572789	-1.74055902	0.486610231
2	0.924386886	DEHA2E15422g		unknown		-1.24095981	-0.34863912	0.970974877
4	0.983607697	DEHA2D01826g		transporter activity	Endoplasmic reticulum vesicle protein 25	**2.222109269**	1.785722238	1.087834078
1	0.982332216	DEHA2E11572g		unknown		0.634721096	1.20193334	**2.128701811**
5	0.741485971	DEHA2E02376g		binding	HDA1 complex subunit 3	**-2.38582364**	-1.65216978	-1.54834006
5	0.949453375	DEHA2E23056g		transporter activity	Boron transporter 1	-1.09389082	-1.14786095	**-2.39859527**
1	0.990881527	DEHA2E21604g		amino acid	Acetolactate synthase small subunit, mitochondrial	1.249643831	1.728102561	**2.361677601**

				metabolism				
2	0.928332019	DEHA2E17578g		unknown		-1.35592241	-0.44500554	0.878442808
2	0.958242494	DEHA2E10538g		unknown		**-2.26481459**	-0.02864415	-0.01149404
1	0.945823033	DEHA2E06974g		transferase activity	Trans-aconitate 3-methyltransferase	0.387802793	1.371255807	**2.252212912**
2	0.936765516	DEHA2E04180g	W	unknown		-1.03831934	-0.1213063	0.982560058
5	0.972616171	DEHA2E02266g	H	ion binding	Aconitate hydratase, mitochondrial	**-2.0808172**	**-3.50705144**	**-3.6669109**
3	0.98263995	DEHA2E09614g		unknown		0.545547148	-1.36867929	0.784423594
6	0.973821308	DEHA2E19228g		unknown		0.205510435	0.455705377	-1.75146962
2	0.968042407	DEHA2E18238g		molecular function		**-2.00904434**	-0.55648299	0.211466586
4	0.887864665	DEHA2A05632g		catalytic activity	Ribonuclease H2 subunit A	**2.21686917**	0.587822641	0.986811103
5	0.941045686	DEHA2E15268g	W	ion binding	Putative transcription factor SEF1	**-2.32806935**	**-3.14768877**	**-2.81493139**
2	0.632164109	DEHA2E18062g		unknown		-0.39733808	1.78050152	0.815545389
4	0.877864939	DEHA2A10076g		protein metabolism	Protein FYV10	**2.208949701**	0.750606319	1.588875405

1	0.935060993	DEHA2E14630g		transporter activity	General amino-acid permease GAP1	1.936416327	**2.714757581**	**2.876292474**
3	0.908369508	DEHA2E15048g		unknown		0.254894077	**-2.49456483**	-0.28678792
1	0.927226236	DEHA2E21384g		catalytic activity	Peptide-N(4)-(N-acetyl-beta-glucosaminyl)asparagine amidase	1.771568708	1.901630352	**2.226747525**
2	0.996663994	DEHA2E22264g	W	unknown		-1.88790241	0.011795685	0.908506014
2	0.718512197	DEHA2E15400g	W	unknown		**-2.23896483**	-0.03445499	-1.05081146
1	0.901135768	DEHA2E11088g		unknown		1.351551447	0.679870701	**2.323242504**
6	0.998421015	DEHA2E04224g	W	unknown		0.214780088	-0.07263884	-1.79570993
1	0.911423416	DEHA2E21164g	W	catalytic activity	Lipase 2	0.731242493	0.666996391	**2.757100336**
1	0.984194776	DEHA2E14300g		unknown		0.92196146	1.81241114	**2.76606082**
2	0.987428454	DEHA2E14696g	W	unknown		-1.31843891	0.368736821	0.881971533
1	0.678412872	DEHA2E09702g		unknown		0.50939186	**2.011533979**	1.195408713
6	0.911386133	DEHA2E06842g		transporter activity	Inorganic phosphate transporter PHO87	-0.27619688	-1.28479365	**-2.69978416**

1	0.909792993	DEHA2E11330g		unknown		0.348567514	0.677219061	**2.32344546**
1	0.91273509	DEHA2F01738g	W	biological process	Protein SYM1	**2.183299657**	**3.302813885**	**3.235706187**
4	0.85879406	DEHA2F20020g		ion binding	Structural maintenance of chromosomes protein 1	**2.175214355**	1.537239155	0.158727532
1	0.975193336	DEHA2E19954g		lipid metabolism	Sphingosine N-acyltransferase LAG1	1.721369376	**2.668875506**	**3.257797756**
5	0.982215321	DEHA2E08888g	H	oxidation-reduction process	Succinate dehydrogenase [ubiquinone] flavoprotein subunit, mitochondrial	-1.40939596	**-2.27067309**	**-2.51160289**
3	0.702186984	DEHA2E15246g	W	unknown		-1.62088384	-1.73996321	0.596867857
1	0.99657569	DEHA2E11924g		unknown		1.100157632	1.570150254	**2.289096311**
6	0.97635484	DEHA2E09768g	H	cell part	Centractin	0.127119378	-0.52170313	**-2.06487136**
4	0.67786633	DEHA2E12804g	H	unknown		1.77763961	0.40655784	-0.48309212
1	0.953538039	DEHA2C14960g		molecular function		**2.10122545**	1.624641751	**3.115796999**
6	0.995906462	DEHA2E18854g	W	transporter activity	Low-affinity glucose transporter HXT3	0.007237965	-0.3983778	**-2.8625022**
1	0.994924729	DEHA2E14190g		unknown		0.883898497	1.129299229	**2.137472574**

4	0.983603008	DEHA2D18722g		ion binding	Replication factor C subunit 5	**2.098485789**	1.219994964	0.87562816
6	0.883839183	DEHA2E01672g	W	unknown		0.590610485	-0.62794854	-1.59149529
6	0.65621553	DEHA2E22352g		unknown		-0.06236588	1.316750043	-0.83620268
6	0.754535576	DEHA2E14080g	W	unknown		1.546495273	1.180116561	-0.53150724
2	0.882299295	DEHA2E08558g		carbohydrate metabolism	2-deoxyglucose-6-phosphate phosphatase 1	-1.01752925	1.430788132	**2.474616978**
3	0.713915549	DEHA2E20328g		unknown		**-2.26226463**	**-3.30382192**	-1.04188073
4	0.930889507	DEHA2F14784g		cell part/ cell assembly	Cell division control protein 31	**2.095288534**	**2.147759922**	1.776440069
2	0.999329923	DEHA2E23980g	H	molecular function		**-2.09757015**	0.085467601	0.692221084
5	0.988607356	DEHA2E07458g	H	oxidation-reduction process	Succinate dehydrogenase [ubiquinone] flavoprotein subunit, mitochondrial	**-2.72332428**	**-3.67772083**	**-4.06920446**
2	0.900404158	DEHA2E15664g		unknown		-1.20295617	0.236129116	1.991084051
5	0.967944158	DEHA2E07392g	W	binding	Nuclear and cytoplasmic polyadenylated RNA-binding protein PUB1	-1.27726027	**-2.01818064**	**-2.00155594**

6	0.944104719	DEHA2E09262g		unknown		-0.32032611	0.27200789	-1.84026302
2	0.994095363	DEHA2E22880g		unknown		-1.61427023	-0.1527304	0.62454245
5	0.83627275	DEHA2E01232g		oxidation-reduction process	Superoxide dismutase	**-2.57475708**	**-2.37753664**	**-2.02274416**
6	0.49691691	DEHA2E06820g		unknown		1.160248281	-1.43736815	-1.10595487
5	0.915150026	DEHA2F05588g	W	molecular function		-1.40208546	-1.01359136	**-2.59728186**
3	0.994021603	DEHA2F08954g	W	unknown		0.443489195	-1.88593316	0.822973861
1	0.998829994	DEHA2F24068g		unknown		1.326815876	1.699790772	**2.978601786**
5	0.951054335	DEHA2F08844g		ion binding	Meiotic mRNA stability protein kinase SSN3	-1.71241349	-1.34444028	**-2.69222752**
6	0.808468311	DEHA2F05148g		unknown		0.231598896	-1.30935933	-1.989365
4	0.861446049	DEHA2E02662g	W	physiological response to stimulus	Cold shock-induced protein TIR1	**2.093535257**	0.842749154	0.19845375
2	0.957474206	DEHA2F26312g	W	unknown		-1.27173716	0.339634348	1.412923647
1	0.990330392	DEHA2F07722g		catalytic activity	Acid phosphatase PHO12	0.973135546	1.604544468	**2.834477424**

1	0.885020336	DEHA2C17600g		binding	Uncharacterized membrane protein YJR124C	**2.064250251**	1.631041155	**2.258310784**
2	0.880105567	DEHA2F13178g		unknown		-1.05387229	0.026363366	1.758118096
6	0.890208083	DEHA2F25300g		unknown		0.835241683	-0.15604935	-1.2007441
6	0.973069525	DEHA2F07788g	W	binding	Uncharacterized protein YMR124W	-0.34056909	-0.60327438	**-2.30512984**
1	0.584635389	DEHA2F06072g	W	cell part/ cell assembly	Spore membrane assembly protein 2	0.079375782	**2.309911014**	1.208301604
5	0.999963229	DEHA2F02552g	H	unknown		-1.34478495	-1.64283448	**-2.17064324**
6	0.835978336	DEHA2F05390g		unknown		-0.7062549	0.375086522	-1.73587442
1	0.879037874	DEHA2A08294g	W	molecular function		**2.064054668**	1.654757773	**2.218217162**
5	0.936050218	DEHA2F12166g	W	cell part	Cell wall protein CWP1	-0.97040347	-1.4109229	**-2.82213982**
3	0.642999252	DEHA2F21846g		unknown		1.578824085	-1.55917466	-0.34823695
6	0.877477643	DEHA2F02112g	H	unknown		1.004916805	-0.26755315	-1.44176416
6	0.928795808	DEHA2F21736g		unknown		-0.6929229	-0.85262119	**-2.40162415**

4	0.882095983	DEHA2B10230g		unknown		**2.062830022**	**2.380817513**	1.998317494
1	0.975983542	DEHA2F01430g		binding	Ribosome biogenesis protein SLX9	0.965387503	1.199752664	**2.786250538**
3	0.906321215	DEHA2F06446g		unknown		0.410437548	-1.97463039	-0.12507978
5	0.996945411	DEHA2F10582g		oxidation-reduction process	Peroxisomal catalase A; Catalase	**-2.13381213**	**-2.54287234**	**-3.14890607**
6	0.98294008	DEHA2F19646g		cell part	Sister chromatid cohesion protein PDS5	0.075938218	0.360727891	**-2.30001019**
1	0.951166348	DEHA2F11044g	W	transferase activity	Uncharacterized protein YMR209C	1.408956306	1.007951975	**2.508468427**
4	0.924774604	DEHA2G18964g	W	cell part/ cell assembly	Cell wall protein DAN4	**2.057974363**	**2.247626537**	1.336224715
3	0.961855211	DEHA2F02706g	W	unknown		0.612409464	-1.07699085	1.162648838
5	0.834406946	DEHA2F04972g		oxidation-reduction process	Sulfite reductase [NADPH] subunit beta	-0.18249763	**-2.25041483**	**-2.96563141**
1	0.79072367	DEHA2F01914g		unknown		1.446176434	0.325294439	**2.054701941**
5	0.936022988	DEHA2F23232g		unknown		-0.99486939	-1.57891465	**-3.03835877**
2	0.934127563	DEHA2F15048g		unknown		-0.99662357	0.8590297	1.136996792

3	0.6833348	DEHA2F00594g	W	unknown		1.452663161	-0.59047404	0.481381414
2	0.877238697	DEHA2F10846g	W	unknown		-0.99250761	1.265339361	1.069146671
2	0.912718414	DEHA2F13354g		unknown		-1.29964625	1.443789778	1.911392012
5	0.979220724	DEHA2F23188g		ion binding	Helicase SWR1	-0.99832084	-1.25368306	**-2.10934907**
3	0.999655309	DEHA2F25982g		unknown		0.160775077	-1.49195521	0.623958046
3	0.956272487	DEHA2F11990g	W	catalytic activity	Steryl acetyl hydrolase 1	-0.45260875	**-2.83482738**	-0.10587876
6	0.986670672	DEHA2F25432g		cell part	Nucleolar pre-ribosomal-associated protein 1	-0.25647141	-0.34421737	**-2.11012045**
3	0.698349575	DEHA2F17248g		unknown		-0.22448967	**-2.33994357**	-1.22071682
1	0.927749067	DEHA2F11550g		transferase activity	Putative alcohol acetyltransferase	0.447767594	**2.254536199**	**4.101741421**
3	0.724321094	DEHA2F19294g	W	cell part/ cell assembly	Flocculation protein FLO11	0.3776412	-0.44217988	**2.993352324**
1	0.996101225	DEHA2F06512g	W	binding	UDP-N-acetylglucosamine transferase subunit ALG14	1.341663244	1.761989072	**3.250110712**
3	0.825986361	DEHA2F01892g		catalytic activity	4-hydroxyphenylpyruvate dixygenase activity	-0.41521618	**-3.34843505**	-1.14471085

5	0.997543521	DEHA2F26708g		unknown		-1.39533911	-1.89060118	**-2.53862364**
6	0.996630155	DEHA2F16126g	W	transporter activity	Uncharacterized vacuolar membrane protein YJR054W	0.162355998	0.128593522	**-2.02065005**
5	0.900140387	DEHA2F20262g	W	transporter activity	Low-affinity glucose transporter HXT3	-1.98210834	-1.21663961	**-2.27250371**
6	0.992078324	DEHA2F21868g		binding	WD repeat-containing protein YDL156W	0.545739992	0.042009375	**-2.36492301**
5	0.911088991	DEHA2F11286g		binding	Bud site selection protein 31	**-2.2761333**	**-2.47027079**	**-2.22722699**
6	0.91505945	DEHA2F06468g	W	biological process	tRNA (cytidine(32)-2'-O)-methyltransferase non-catalytic subunit TRM732	-0.64635441	0.365627231	**-2.47197872**
3	0.846895574	DEHA2F00770g	W	unknown		-0.67812889	-1.25823689	0.894557303
3	0.936387552	DEHA2F11704g		protein metabolism	Probable E3 ubiquitin-protein ligase HUL4	-0.26954484	**-2.49635955**	-0.26954484
1	0.953146223	DEHA2F02948g		oxidation-reduction process	Putative reductase 1	0.558953156	1.67763077	**2.402920942**
6	0.986729057	DEHA2F05676g		ion binding	ATP-dependent helicase ULS1	0.536925233	-0.21877912	**-2.49401225**
2	0.734275772	DEHA2F05566g	W	transporter activity	High-affinity methionine permease	**-2.06305755**	-0.67239694	-0.98377744
3	0.830886928	DEHA2F00110g		unknown		-1.69198686	**-3.10081417**	-0.52552848

6	0.937035938	DEHA2F08602g	W	ion binding	Putative serine/threonine-protein kinase YPL150W	-0.62246009	-1.23941552	**-3.17393827**
6	0.951498989	DEHA2F13310g	W	binding	DASH complex subunit DAD3	-0.2680585	-0.80849475	**-2.21820863**
5	0.935849871	DEHA2F14916g		protein metabolism	N-terminal acetyltransferase A complex subunit NAT5	-1.06128107	-0.93619969	**-2.15142163**
5	0.917515969	DEHA2F17754g		oxidation-reduction process	Cytochrome c peroxidase, mitochondrial	**-2.40477104**	**-3.31795919**	**-2.75237732**
5	0.795968378	DEHA2F04444g		transporter activity	Related to na+/k+/2cl-cotransporter	-1.87278834	-0.61798802	**-2.52274952**
3	0.713055005	DEHA2F17644g		unknown		1.36297508	-1.04475386	0.150697882
5	0.926520292	DEHA2F08888g		protein metabolism	Porphobilinogen deaminase	-1.93332321	**-2.75267091**	**-2.33147936**
6	0.853558657	DEHA2F23958g		binding		-0.19122027	-1.56659328	**-2.62727706**
6	0.951511154	DEHA2F27258g		molecular function		0.329508368	-0.69173295	**-2.22973185**
2	0.950173647	DEHA2F19580g		unknown		**-2.18681272**	-0.24162611	-0.13429004
6	0.887114779	DEHA2F12694g	W	unknown		0.342054302	-0.92221651	-1.93828536
2	0.907838959	DEHA2F19470g	W	unknown		-1.95438695	-0.93232723	0.060487912

2	0.690298422	DEHA2F26466g	W	binding	Sequence-specific DNA binding transcription factor activity	**-2.6495148**	**-2.66069187**	0.810734114
5	0.891511611	DEHA2F25894g		unknown		-1.82591201	-1.02658378	**-2.46710541**
2	0.687596725	DEHA2F26356g		unknown		-1.46050933	0.930622228	-0.38289772
5	0.650622535	DEHA2F21230g		unknown		**-2.2583748**	**-2.38036747**	-1.19491725
3	0.775660959	DEHA2F07656g		unknown		0.509727273	-1.52791791	-0.42021714
3	0.866063524	DEHA2F11792g	W	cell part	[PSI+] induction protein 2	-1.08238097	**-3.7028871**	-0.98031685
4	0.792415058	DEHA2A00638g		transporter activity	Lysine-specific permease	**2.057560856**	0.192966589	0.602099725
2	0.984948517	DEHA2F07106g		unknown		**-2.14143628**	-0.3217572	0.931108518
2	0.794459742	DEHA2F05962g		transferase activity	Cation transport regulator-like protein	**-3.40395109**	-1.27163213	-1.30042844
3	0.727521354	DEHA2F12958g		unknown		-1.00958364	-1.17060379	1.062288711
6	0.978284082	DEHA2F23870g		unknown		0.116709578	0.487985404	**-2.50305545**
1	0.982390985	DEHA2F05742g		amino acid metabolism	Histidinol-phosphate transaminase	1.59129854	**2.235168832**	**2.865317566**

3	0.679467843	DEHA2F12738g		unknown		-0.45637709	-0.57535483	1.67659085
2	0.946671909	DEHA2F25938g	W	ion binding	Serine/threonine-protein kinase KSP1	**-2.04241769**	0.315141706	0.101300798
5	0.937153681	DEHA2F20812g		oxidation-reduction process		-0.59197612	-1.38370106	**-2.06019506**
5	0.938227543	DEHA2F08360g	H	binding	NUBM protein	-1.11251981	**-2.50506633**	**-3.82960721**
1	0.979780665	DEHA2G05082g		oxidation-reduction process	Iron transport multicopper oxidase FET3	**2.050486172**	**3.485285461**	**4.425896521**
3	0.986953962	DEHA2F02046g		unknown		0.41491056	-1.2347924	0.854082257
2	0.921255277	DEHA2F05412g		unknown		-1.22385902	1.201737558	1.881444943
5	0.90209736	DEHA2F10120g	H	oxidation-reduction process	NUCM protein	-0.46239658	-1.21518444	**-2.18247554**
3	0.681328629	DEHA2F09746g		molecular function		0.072469985	**-2.34420275**	-1.22794001
2	0.934271182	DEHA2F14344g	W	unknown		-1.76807332	0.609870485	0.290596104
6	0.866558611	DEHA2G17358g		unknown		-1.15000962	-0.38162354	**-2.43328386**
1	0.934645333	DEHA2G08624g		molecular function		1.835822123	1.250776561	**2.665915291**

3	0.948044625	DEHA2G03894g		unknown		0.761929537	-1.0013709	1.214492689
2	0.914817107	DEHA2G07634g		molecular function		**-2.09035206**	-0.99759964	0.309301461
2	0.987596223	DEHA2G10142g	W	unknown		-1.94917841	-0.30223574	0.314961559
3	0.716128285	DEHA2G11990g		unknown		-0.9415606	-1.0800933	1.269644792
3	0.978105226	DEHA2G13398g	W	unknown		0.758314192	-1.77417415	1.47560183
2	0.984605136	DEHA2G04664g		unknown		**-2.20489824**	-0.0521558	1.370780194
3	0.819453035	DEHA2G18018g		transporter activity	Mitochondrial import inner membrase translocase subunit TIM13	-0.90673654	**-2.02530523**	-0.59861918
6	0.960347453	DEHA2G12298g		biological process	Protein MUM2	-0.42922515	-0.69166021	**-2.28207457**
2	0.589903323	DEHA2G19756g		protein metabolism	Protein disulfide-isomerase MPD1	**-2.07300854**	1.532286084	-0.85866263
5	0.915700289	DEHA2G15510g		transporter activity	Probable transporter MCH4	-0.79001063	-1.17182658	**-2.56440041**
6	0.971877747	DEHA2G21384g		unknown		0.636887284	0.062837944	-1.59212896
1	0.943086126	DEHA2G24387g		binding	Bud site selection protein BUD4	1.240667113	0.93972055	**2.928477194**

1	0.755050935	DEHA2G18656g		unknown		-0.18665274	**2.236004234**	**2.097630038**
5	0.999456537	DEHA2G24024g	W	physiological response to stimulus	Guanine nucleotide-binding protein subunit gamma	-1.51758581	-1.92384974	**-2.45039959**
3	0.983432041	DEHA2G13420g		unknown		-0.13469119	-1.79626922	0.937177688
1	0.939298839	DEHA2G08822g	H	amino acid metabolism	Phospho-2-dehydro-3-deoxyheptonate aldolase, phenylalanine-inhibited	0.428530801	0.71638286	**2.02280402**
4	0.903555644	DEHA2E22770g		binding	Karyogamy protein KAR4	**2.043435222**	1.761025307	0.500239063
1	0.776788383	DEHA2G02244g		molecular function		1.303177119	**2.078259622**	1.503457224
2	0.919143336	DEHA2G19360g	H	unknown		-0.85587413	0.21095738	1.28592072
5	0.989888822	DEHA2G24728g		transporter activity	Oligomycin resistance ATP-dependent permease YOR1	-1.48144389	-1.80632594	**-2.83811395**
6	0.985503685	DEHA2G20064g	W	transporter activity	Mitochondrial inner membrane protein COX18	-0.14951177	-0.58765218	**-2.63931249**
6	0.91393067	DEHA2G18370g		unknown		-0.8795162	-0.25075196	**-2.37723617**

2	0.783629016	DEHA2G01144g	W	unknown		-0.77087921	1.287917817	0.657947215
3	0.771465943	DEHA2G20878g		transferase activity	ADR347C	-1.58918283	**-3.02427286**	-1.03241776
6	0.867139092	DEHA2G04862g		unknown		-0.94646253	-0.12541999	**-2.08433102**
5	0.974596163	DEHA2G18260g	H	unknown		-0.99635363	-1.64088486	**-2.43497603**
1	0.983347372	DEHA2G10230g		unknown		1.192969484	1.141422217	**2.404966927**
1	0.959242788	DEHA2G16280g	W	catalytic activity	Putative peptidase YMR114C	0.996844996	0.833402235	**2.255307729**
3	0.948710417	DEHA2G11110g		unknown	Uncharacterized protein YIL067C	0.585595487	-1.66717748	0.32005124
1	0.826267927	DEHA2G05632g		cell part/ cell assembly	Uncharacterized protein YIL067C	-0.08762392	0.3720516	**2.130201233**
1	0.976783186	DEHA2G22572g		amino acid metabolism		0.74343418	1.184275371	**2.502707762**
4	0.774959176	DEHA2C02860g	W	molecular function		**2.037174795**	0.143758904	0.487622789
6	0.899994251	DEHA2G12276g	H	molecular function		-0.43854799	-1.35625893	**-2.72620039**
6	0.928992982	DEHA2G22308g		unknown		0.58860899	-0.34657786	-1.49363741

6	0.889296382	DEHA2G01562g		unknown		-0.5917684	0.366917446	-1.95281198
5	0.989814136	DEHA2G13090g	W	binding	Sequence-specific DNA binding	-1.36124531	**-2.08051661**	**-2.79378645**
3	0.704114796	DEHA2G21252g		oxidation-reduction process		0.039911672	**-2.79078781**	-1.38398057
2	0.968202194	DEHA2G07568g		unknown		-1.73136024	0.539630405	0.532658947
5	0.848875588	DEHA2G21208g		molecular function	Essential protein involved in cytokinesis	-1.08557807	**-2.26939007**	-1.57578569
5	0.996047349	DEHA2G23980g		molecular function		-1.61978552	-1.74160528	**-2.45853694**
1	0.835802761	DEHA2G22946g		unknown		-0.20272802	0.636435265	**2.047866067**
5	0.938703758	DEHA2G24750g		ion binding	Adenosylmethionine-8-amino-7-oxononanoate aminotransferase	-1.30139404	-1.54286299	**-3.28757476**
2	0.904749207	DEHA2G04950g	W	unknown		-1.89732964	-0.85337149	1.033756914
1	0.938116713	DEHA2G23760g		molecular function		0.782609239	**2.219215992**	**2.641284833**
1	0.908706799	DEHA2G07238g	H	oxidation-reduction process	Heme oxygenase	0.484275508	1.794318534	**2.017582244**
5	0.986636794	DEHA2G02970g		ion binding		-1.50561729	-1.57605477	**-2.59655404**

1	0.962636193	DEHA2G08118g	W	transporter activity	Syntaxin PEP12	0.863422022	1.41812997	**3.345402934**
4	0.981390326	DEHA2C17182g	W	ion binding	E3 SUMO-protein ligase MMS21	**2.029719516**	1.520747299	0.874433129
5	0.983517796	DEHA2G20790g		cell part	Uncharacterized protein YGR266W	-1.65791049	**-2.00414674**	**-2.20623966**
2	0.890728466	DEHA2G15334g	W	unknown		-0.75288216	0.769592116	1.734805467
5	0.648337768	DEHA2G00990g		molecular function		0.01592036	**-2.14840357**	-1.28704644
1	0.980582853	DEHA2B09614g		cell part/ cell assembly	Uncharacterized protein YPL066W	**2.010231923**	1.822522934	**3.683567122**
1	0.951281964	DEHA2G07986g		transporter activity	Copper-transporting ATPase	0.69814684	0.795057079	**2.290960813**
1	0.974479247	DEHA2G05192g	H	binding	Small nuclear ribonucleoprotein E	1.492370752	1.422287429	**2.265320255**
6	0.944875536	DEHA2G05148g	W	unknown		0.014513666	0.580522397	-1.74577729
2	0.990344873	DEHA2G22088g		transporter activity	Uncharacterized mitochondrial carrier YMR166C	**-2.44980868**	-0.28168823	0.405893627
1	0.987791186	DEHA2G22550g		amino acid metabolism	Low specificity L-threonine aldolase	1.028500939	1.83906657	**2.609791286**
6	0.848769882	DEHA2C07524g		molecular function		**2.005308325**	0.87032472	-1.40455294

1	0.940647913	DEHA2G08756g		transferase activity	DNA polymerase epsilon subunit D	1.619475211	1.742204144	**2.122243449**
6	0.595957468	DEHA2G13244g	W	unknown		-0.9560028	0.900457228	-1.33377633
2	0.668104594	DEHA2G16918g	W	transferase activity	Protein farnesyltransferase subunit beta	**-2.03404144**	-1.58029809	-0.71721811
5	0.920452149	DEHA2G15928g		oxidation-reduction process	Succinate dehydrogenase [ubiquinone] cytochrome b small subunit, mitochondrial	-1.97763435	**-4.31022361**	**-3.84479024**
3	0.989321784	DEHA2G06666g		unknown		0.368082131	-1.8878108	1.299089775
5	0.971002084	DEHA2G18194g	H	binding	Exosome complex component SKI6	-0.99063295	-1.88625125	**-2.33919016**
3	0.99732977	DEHA2G15818g	W	unknown		0.024130909	-1.79183246	0.778137631
5	0.688501441	DEHA2G18084g	W	unknown		**-2.39399106**	-0.62478435	**-2.12341466**
3	0.899197992	DEHA2G16632g		unknown		0.719560889	-0.9441792	1.966989179
3	0.905280119	DEHA2G03696g	W	binding	Protein CWC16	0.860785802	**-2.12872265**	0.15393726
5	0.962340628	DEHA2G15642g		unknown		-1.82994351	**-3.05857928**	**-2.99075077**
3	0.816551504	DEHA2G14652g		molecular function		1.144146933	-0.46747427	**2.442051543**

2	0.885912504	DEHA2G19778g	W	unknown		-0.93961478	-0.11081032	1.317187806
4	0.784989057	DEHA2E12518g		unknown		**2.004365547**	0.423055256	1.59249383
1	0.9508238	DEHA2G17402g	W	transporter activity	Vacuolar basic amino acid transporter 1	0.914323921	0.743608718	**2.183432298**
6	0.974846677	DEHA2G13552g	W	catalytic activity	Altered inheritance of mitochondria protein 6	0.760553805	0.476164043	**-2.00392513**
5	0.964299831	DEHA2G12518g	H	ion binding	Translation initiation factor RLI1	-1.92179013	**-3.01891486**	**-2.93587845**
5	0.974929654	DEHA2G06050g		oxidation-reduction process	NUAM protein	-1.792342	**-3.27733821**	**-4.16806112**
3	0.847959849	DEHA2G09724g		catalytic activity	Similar to putative intramembrane serine proteases	-0.9846388	**-2.60005305**	-0.70816583
5	0.925401027	DEHA2G19382g	H	oxidation-reduction process	Succinate dehydrogenase [ubiquinone] iron-sulfur subunit, mitochondrial	**-3.19905524**	**-5.19857896**	**-4.36775361**
5	0.990918286	DEHA2G24794g		transporter activity	Choline transport protein	-1.19072672	-1.83761421	**-2.30108337**
5	0.648071404	DEHA2G16940g	W	protein metabolism	Tyrosine-protein phosphatase 2	-0.04815705	**-2.79946996**	-1.61982199